Progess in superhydrophobic surface development

Paul Roach, Neil J. Shirtcliffe* and Michael I. Newton

Research into extreme water-repellent surfaces began many decades ago, although it was only relatively recently that the term superhydrophobicity appeared in literature. Here we review the work on the preparation of superhydrophobic surfaces, with focus on the different techniques used and how they have developed over the years, with particular focus on the last two years. We discuss the origins of water-repellent surfaces, examining how size and shape of surface features are used to control surface characteristics, in particular how techniques have progressed to form multi-scaled roughness to mimic the lotus leaf effect. There are notable differences in the terminology used to describe the varying properties of water-repellent surfaces, so we suggest some key definitions.

Introduction

Some superhydrophobic surfaces can cause water and even oils to roll off leaving little or no residue and carry away any resting surface contamination. With more and more researchers becoming interested in this field there are a greater number of methods reported to produce such surfaces, using simpler and cheaper means to achieve high water-contact angles (WCAs) and low hysteresis (causing roll-off). The number of articles on superhydrophobic surfaces published between 2006 and 2007 is more than double the total number of articles published previously, demonstrating a high level of interest in this area for all manner of uses; from self cleaning, anti-fog or anti-corrosion surfaces to basic research. A number of reviews covering this subject area have previously been published;[1] some detailing a more specialised sub-set of topics.

School of Biomedical and Natural Sciences, Nottingham Trent University, Clifton Lane, Nottingham, UK NG11 8NS. E-mail: neil.shirtcliffe@ntu.ac.uk; Fax: +44 (0)115-848-6636; Tel: +44 (0)115-848-8062/3315

Michael I. Newton

Dr Michael I. Newton, is a reader in experimental physics in the Division of Physics and Mathematical Sciences at the Nottingham Trent University. Following his physics degree in 1983 (BSc, Hons) he obtained an MSc in modern electronics and a PhD in semiconductor physics at the University of Nottingham. Since becoming a lecturer at the Nottingham Trent University, he has developed lithographic facilities for surface acoustic wave device fabrication, which he has now extended to include thick-film photoresist techniques of patterning surfaces for wetting applications. His research interests include the development of surface acoustic wave systems and the investigation of wetting processes on solid surfaces.

Paul Roach

Dr Paul Roach received his first degree in chemistry (MChem) in 2002 from the Nottingham Trent University, and subsequently a PhD in chemistry in 2005 for his research of protein–surface interactions. Currently a post-doctoral research fellow at the university, Paul is investigating the development of Love wave-sensing devices. His research interests include the design of surfaces for biomedical use and superhydrophobic treatments as anti-fouling surfaces.

Dr Neil J. Shirtcliffe received a BSc (Hons) in chemistry in 1993 and later a PhD in electrochemistry in 1997 from Imperial

Neil J. Shirtcliffe

College, London. His PhD involved measuring electro-deposition of colloids using a QCM. He then worked in Germany at the University of Nuremberg Erlangen, and the Max Planck Insitut fuer Eisenforchung in Duesseldorf where he developed plasma polymer coatings for the protection of steel. In 2001 Neil was appointed as a postdoctoral research fellow at the Nottingham Trent University, where he has been instrumental in combining the chemical aspects of designing super-hydrophobic surfaces with lithographic techniques. Neil's research interests include unusual aspects of superhydrophobicity.

Whilst the basic ideas of superhydrophobicity were developed by Wenzel[2] and Cassie and Baxter[3] decades ago and examples were observed before that, it was a publication in Langmuir by Onda *et al.*[4] that marked the start of an explosion in the of number of articles published on this topic. In 1999 the first critical review was given by McCarthy *et al.*[1b], which was built upon by Callies and Quéré in 2005,[1c] Ma and Hill in 2006[1g] and most recently by Reinhoudt *et al.*[5] Here we give a concise review of the techniques used to prepare superhydrophobic surfaces, where they started and how they have developed over the years up to present day, concentrating on the most recent publications. Extrand[1j] gives a concise overview in a volume of a book series, which we highly recommend as it focuses more on theoretical aspects and therefore compliments this review.

Highly water-repellent surfaces (super-hydrophobic, ultra-hydrophobic) are biologically inspired with the lotus leaf being the classic example.[6] Surface texture, or roughness, is used to enhance the intrinsic hydrophobic chemistry of the surface, producing highly non-wetting surfaces. Superhydrophobic surfaces exhibit extreme water-repellency, with water droplets resting on them with high contact angles.

Various applications benefit from non-wetting surfaces with some specific products becoming commercially available, although the underlying principles behind and effects of superhydrophobicity are still hotly disputed. Currently there are massive parallel efforts to resolve both the principle understanding of wetting and to define methodologies to fabricate superhydrophobic surfaces on small and large scales; for research and mass production, respectively. There are therefore many different routes reported for the production of such surfaces, allowing a vast range of materials to be used as substrates, or modified to give superhydrophobic surfaces. The surface and bulk properties of the material must be taken into account when deciding on a suitable method of preparation. Is the superhydrophobic coating required to be optically transparent, electrically conductive, strong, tough, hard, flexible *etc.*? Can this method be used to produce a conformal superhydrophobic coating on any sized/shaped sample?

Hydrophobicity is usually determined by measuring the contact angle of a water droplet contacting a surface. The angle between the surface and the water meniscus near the line of contact, measured through the droplet, gives an indication of the wettability of the surface (although the size of the drop can affect the outcome). There is usually a difference between the angle produced as the volume of the drop is increased (the advancing angle) and that when it is decreased (the receding angle). This difference, termed the contact-angle hysteresis, gives a measure of the surface 'stickiness'. The greater this difference (larger hysteresis) the more water drops will stick to the surface. Usually low hysteresis is desired when dealing with superhydrophobic surfaces as this means water droplets will roll off extremely easily. Theoretical equilibrium angles lie between the advancing and receding angles, sometimes being determined by vibrating the drop.

The principles of superhydrophobicity were first outlined by Wenzel in 1936[2] and then by Cassie and Baxter in 1944.[3] Wenzel suggested that if liquid contact followed the contours of a rough surface then the effect of roughness should be to emphasise the intrinsic wetting tendency towards either film formation or enhanced contact angle. The contact angle observed on this type of surface is given by Wenzel's equation,

$$\cos\theta_e^W = r\cos\theta_e \qquad (1)$$

where the roughness factor $r > 1$ is the ratio of the true surface area of the solid to its horizontal projection and θ_e is the equilibrium contact angle on a smooth flat surface of the same material. The contribution from the roughness is contained within r and the effect of surface chemistry in θ_e, Fig. 1(a).

However, it can be energetically favourable for a liquid to bridge across the tops of surface features so that the droplet rests upon a composite surface of flat solid tops and flat air gaps between them, as described by the Cassie–Baxter relationship, Fig. 1(b). The contact angle is then given by a weighted average of the cosines of the contact angles on the solid and air using,

$$\cos\theta_e^C = \varphi_s(\cos\theta_e) + (1 - \varphi_s)\cos\theta_X \qquad (2)$$

where $\varphi_s < 1$ is the fraction of the surface present at the tops of the surface protrusions, and $(1 - \varphi_s)$ is the fraction that corresponds to the air gaps, θ_X is the contact angle on the gas in the gaps which is taken to be 180°. This always leads to an increase in contact angle when the droplet bridges the gaps. If they become filled with water θ_X becomes 0°, and the contact angle decreases below that of a flat surface. This second case is not the same as the Wenzel case as the roughness must be filled with liquid before the drop reaches it. This may occur on surfaces with contiguous pores, such as soils or sol–gels, where filling from below or rapid internal spreading (if contact angle allows) can occur. The two equations can be combined to produce a more general equation (eqn (3)) to cover the case when the contacting areas themselves are not flat (Fig. 1(c)).

$$\cos\theta_e^{CW} = \varphi_s r(\cos\theta_e) + \varphi_s - 1 \qquad (3)$$

Additional surface roughness will therefore impact on any liquid contact angle, with angles greater than 90° on a flat surface always increasing (except for the unusual case of pre-existing ponds in the roughness) and those less than 90° potentially moving in either direction. Usually surfaces following the total wetting Wenzel regime are "sticky" in that drops of water tend to adhere to them more than a flat surface of the same type; those following the regime of Cassie and Baxter are "slippy" and allow drops of water to roll off more easily than an equivalent flat surface.[7] It is, however, possible to generate "sticky" surfaces in the regime of Cassie and
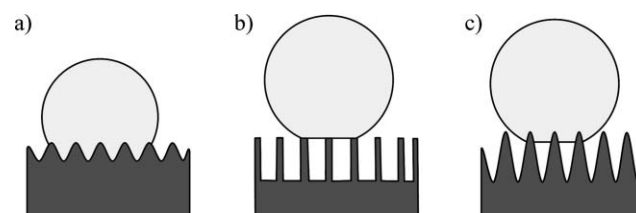

Fig. 1 Wetting states (a) Wenzel, (b) Cassie–Baxter and (c) combined models.

Baxter,[8] usually by using a surface with high intrinsic contact-angle hysteresis; the combined Cassie–Baxter/Wenzel state can also have large hysteresis as the interfacial area between solid and liquid can be at least as large as on a flat surface.[9] For this reason contact-angle hysteresis is not a measure of the wetting state of the surface. Many surfaces show Cassie–Baxter bridging and allow water to roll off if tilted slightly, but water drops falling from a height fill the roughness and may become stuck. The resistance of the transition from a bridging Cassie–Baxter to a wetted Wenzel state depends on the intrinsic chemical hydrophobicity of the surface and the distance between and shape of roughness features. Water condensing onto superhydrophobic surfaces usually ends up in the fully wetting state, although a transition to a bridging state is possible. On surfaces with simple roughness the two states are easy to define, but multilayered or complex roughness can allow a mixture of the two equations to apply;[8] on these surfaces it is often difficult to determine values for r and φ.

The two states are usually considered to be separate energy minima with an energy barrier between. Depending upon the shape of the surface features this energy barrier can be large enough to prevent spontaneous transfer into the primary minimum. Surfaces that are patterned with pillars often show this, with drops deposited on the surface remaining in the Cassie–Baxter state, balanced on the pillars but drops condensing on the surface remain in the Wenzel state. External energy, such as vibration or electrical energy can be applied to transfer drops from one state to another.

Developments in theoretical approaches to problems in superhydrophobicity have occurred in the last 5–10 years,[9] with particular attention being given to using theory to optimise design and to predicting whether a given surface will result in Cassie–Baxter or Wenzel wetting under different conditions. Generally, surfaces are modelled as some kind of periodic array in 2 or 3 dimensions and the free energy (global and/or local) calculated, finite element and lattice Boltzmann analysis have been used for this in some cases, particularly for 3D systems. Such models can reveal the height of the energy barrier between states and whether conversion at a single point will spread or not. Examples of this are given in the work of Kusumaatmaja and Yeomans[9a] and a recent paper by Li and Amirfazli.[9b] Marmur has often focussed on the metastable states of superhydrophobicity in his calculations.[9c] Extrand has investigated the effect of sharp edges on features and of the contact line on superhydrophobicity.[9d] Another focus of research has been to link experimental results with theory; apart from our efforts in this regard notable contributions have been made by Patankar et al. (e.g. investigating contact-angle hysteresis);[9e] Gao and McCarthy (e.g. contact-angle hysteresis)[9f] and Bormashenko et al. (e.g. transition between wetting states)[9g] as well as Quéré and his group (e.g. contact-angle hysteresis).[7] These are just a small selection of the articles published recently. Currently theoretical papers are keeping pace with experimental papers, with each new experimental finding being theoretically tested and integrated into calculations. We have kept this section relatively short as our focus is on materials development; those with a deeper interest can find longer reference lists for theory in other recent reviews.[1j,5]

Originally any surface with a water-contact angle greater than the maximum observable on a flat surface ($\approx 120°$ for PTFE) was considered to be "ultrahydrophobic", but this term and its definition have changed and many recent papers use a minimum of 150° to define a "superhydrophobic" surface with some requiring "low" contact-angle hysteresis in addition. This is critical for many applications as low hysteresis is the basis of most of the useful effects of superhydrophobicity. A similar problem exists on roughened hydrophilic surfaces with some claiming that a contact angle of 0° is sufficient to define a superhydrophilic surface; this is confusing as flat surfaces can exist with this contact angle.

There are therefore many categories of surface where roughness enhances contact angle and not enough official names to define them. We would suggest that if the contact angle is increased by additional roughness but is less than 120° it should be described as positive contact-angle enhancement (as opposed to negative contact-angle enhancement towards zero), currently there is no term for this effect. If the contact angle is increased by roughness to greater than 120° the term ultrahydrophobicity should be used and if the contact angle is increased to greater than 150° and the contact-angle hysteresis is less than $\sim 10°$ the term superhydrophobicity should be used. At this stage there are many reports using whatever terminology comes to mind, making it unclear as to exactly what type of surface is being dealt with, although the last two terms are beginning to attain the meanings suggested here by popular consensus. In this review of current literature we will therefore use the term superhydrophobicity to encompass all types of surface displaying "positive water contact angle enhancement", although most of the recent examples also have low contact-angle hysteresis.

Biologically inspired

A systematic study of water repellency in plants was undertaken by Barthlott and Neinhuis,[6,10] who highlighted the lotus leaf (Nelumbo nucifera) for its super water-repellency and self-cleaning ability, Fig. 2(a). Investigation showed that two scales of waxy surface texture gave rise to the observed effect. Water bridges over the surface roughness in a Cassie–Baxter wetting state allowing it to roll off easily and remove any debris from the surface. They coined the term the lotus effect™, which is now patented as an idea and a trade mark.[13]

There have been several attempts to directly use biological structures as templates for the production of superhydrophobic surfaces, with much interest geared towards various plant leaves, Fig. 2(b), but Barthlott et al. also looked at a variety of insects for similar hydrophobicity,[11] Fig. 2c, and several attempts to directly imprint from these have been reported, most notably the wings of the cicada (Cicada orni).[14] Lichen, mould and fungus have also been shown to have superhydrophobic character, Fig. 2(d).[12]

Other researchers have focused on producing superhydrophobic surfaces via top-down or bottom-up generation of roughness and then using either the intrinsic hydrophobicity of the material or coating the rough surface with a hydrophobic layer. A plethora of techniques have been developed to produce a variety of shaped surface features on different
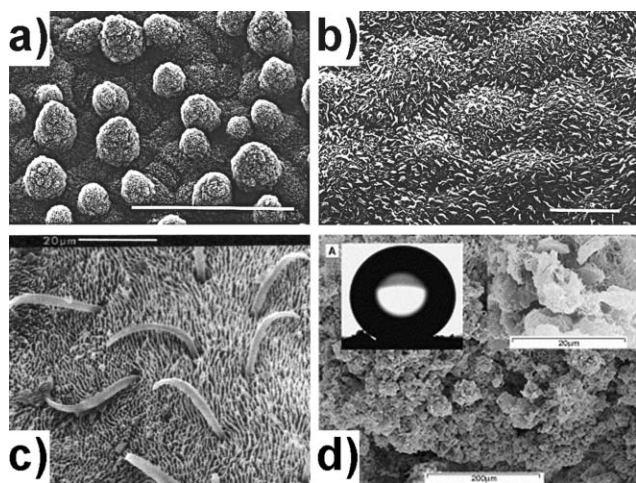
Fig. 2 Superhydrophobic surfaces in biology a) lotus leaf (*Nelumbo nucifera*),[10] b) hillock bush leaf, (*Melaleuca hypericifolia*),[10] c) middle of upper side of a common pond skater (*Gerris lacustris*)[11] and d) the lichen *Lecanora conizaeoides* showing high roughness with inset showing water drop WCA 155 $\pm$ 4°.[12] Images reprinted with permission from (a) and (b) Oxford University Press, Copyright 1997, (c) Blackwell Publishing, Copyright 1996 and (d) Elsevier, Copyright 2006.

length scales, using various materials from polymers to metals. Many routes to prepare superhydrophobic surfaces require complicated, sometimes expensive equipment, although some surfaces can be fabricated fairly easily. Here we describe how the preparative methods of superhydrophobic surfaces, both the substrates and any applied over-layers, have increased in number and been developed over the past years.

Fibres and textiles

The problem of waterproofing surfaces, specifically for fabrics, was first critically examined by Wenzel in 1936.[2] Superhydrophobic surfaces can be produced simply by making woven or non-woven cloth hydrophobic without altering its roughness. As the roughness of the cloth is usually on a relatively large scale, some efforts have been made to generate smaller scale structures to increase the superhydrophobicity and pressure resistance of the structures.

A patent published in 1945 detailed the use of an alkyl silane to hydrophobise paper or fabrics.[18] The silane reacts with moisture in the fibrous material, allowing it to hydrolyse and condense to form a hydrophobic layer. Gao and McCarthy have recently demonstrated that this method can be used for the production of an 'artificial lotus leaf' using polyester textiles as substrates,[19] although the term 'superhydrophobic' (or any variant thereof) does not appear in the original patent. Zhang *et al.*[20] reported the production of a superhydrophobised cotton fabric by plasma coating it with a perfluorocarbon layer. In wash cycle tests these plasma-coated samples performed better than others treated with Scotchguard™. Daoud *et al.*[21] further developed the silane-coating method, again using a silane with an alkyl group to present a hydrophobic character, but also having a glycidyl functional group allowing the formation of a strong bond between the

coating and the surface groups of the cotton fibres. This gave a superhydrophobic surface with increased durability.

In 2006, Liu *et al.* reported artificial lotus leaf structures on cotton textiles using carbon nanotubes (CNT).[16] Cotton fibres were shown to be covered with nanoscale roughness after being dipped into a CNT suspension, Fig. 3(c), with poly(butyl acrylate)-modified CNTs showing another level of roughness. Fabric surfaces treated with either coating were found to be superhydrophobic, Fig. 3(e). Pulsed laser deposition of thin Teflon® films were also shown to convey additional nanometre-sized granular roughness to cellulose fabrics,[22] and similarly the impregnation of cloths with gold particles (Fig. 3(d)), which were further functionalised, gave superhydrophobic surfaces.[17] Michielsen and Lee[15] have recently reported the surface modification of woven nylon (Fig. 3(a)), achieving an apparent WCA of 168°.

Single fibres, as well as woven materials, have been produced to give an extra degree of roughness to the fibre surface which, along with various hydrophobic chemical coatings, has afforded superhydrophobic surfaces. The main concern in the area of fabric-related superhydrophobic/self-cleaning surfaces is the retention of their properties with use. Surfaces which do not have inherent hydrophobic properties or multiscale roughness require additional coatings, which
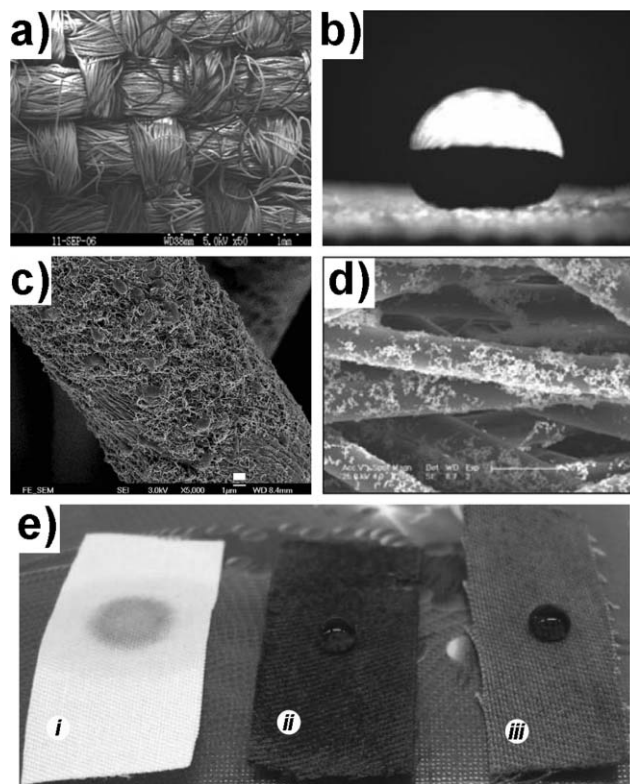

Fig. 3 Woven superhydrophobic surfaces (a) multifilament woven fabric,[15] (b) droplet resting on surface shown in (a), (c) CNT-treated cotton fibre,[16] (d) cloth surface impregnated with gold particles,[17] and (e) water droplets on[16] i) untreated woven cotton sheet, ii) CNT-treated woven cotton sheet shown in (c) and iii) poly(butyl acrylate)–CNT-treated woven cotton sheet. Images reprinted with permission from (a) and (b) American Chemical Society, Copyright 2007, (c), (d) and (e) The Royal Society of Chemistry, Copyright 2007.

may become damaged or diminish with frictional wear or repeated washing cycles.

Production of synthetic filaments with the aid of electrostatic forces is known as electrospinning. Electrospun fibres can be very small, but tend only to be available as non-woven mats. However, this method of fibre production has received much interest due to the fibre size, surface texture and composition along the fibre length and the wide variety of polymers that can be used. The reduced degradability of electrospun fibre mats compared to cast polymers also made them appealing to the medical/biomaterials industry.[28] In 1994, Reneker and Dzenis proposed a new method for the production of continuous oriented fibres of both synthetic and natural polymers by electrospinning.[29] These fibres had diameters ranging from 50 nm to several microns. The technique has been developed to produce smaller fibres, with more and more materials being used and various cross-sectional shapes being reported.[30]

In 2004, it was found that the wettability of mats made from smaller diameter electrospun fibres was decreased.[31] As might be expected for rough and hydrophobic surfaces, electrospun surfaces showed excellent water repellancy.[32] The self-cleaning properties of these surfaces were discovered by Menceloglu et al. with a WCA of 172° and very low hysteresis being reported.[33] Dust- and stain-resistant surfaces were suggested using poly[bis(trifluoroethoxy)phosphazene] spun fibres.[34] Trifluoroethoxy polyphosphazene was reported to be one of the most hydrophobic polymers; resistant to oils and having high radiation stability they had obvious applications in biomedical and advanced materials. Ma et al. reported the superhydrophobicity of an electrospun block copolymer (poly(styrene-block-dimethylsiloxane)), showing that the water repellancy was due not only to the chemistry of the surface and the structure of the fibrous mat, but also to the distinct phase segregated nature of the fibres, Fig. 4(a).[23] Agarwal et al. reported the electrospinning of a range of fluorinated homo- and co-polymers to produce a variety of textured surfaces, Fig. 4(b).[24] By changing the process conditions fibres ranging from uniform cylinders to globules were formed, with some nano-fibres being connected by micro-particles. Similar morphologies were observed for polystyrene spun fibres, Fig. 4(e), although it was observed that some of the connecting particles were often removed from the surfaces by water.[27] This problem was solved by spinning a secondary layer of fibres over the initial fibre-particle surface. Block copolymer electrospinning has also been shown to result in fibres having concentric ring or aligned core–shell microphases.[35] These types of fibres, having internal self-assembled structures, may be useful in tuning material properties whilst controlling the external surface chemistry.

Micro-/nano-porous fibres biologically inspired to imitate the self-cleaning properties of the silver ragwort leaf were formed by carefully controlling the solvent during electrospinning polystyrene.[36] Nanostructured pores were created in the fibres, with fibrous mats having WCAs of nearly 160°. Ma et al. have also shown higher contact angles and lower hysteresis using fibres 'decorated' with nanometre-sized pores or particles, Fig. 4(c).[25] Ogawa et al. reported the use of an additional particle layer on cellulose acetate fibres.[26] After electrospinning, the fibres were treated with a layer-by-layer deposition of poly(acrylic acid) and TiO_2 particles and the resulting rough fibre structure was fluorinated to give a superhydrophobic surface, Fig. 4(d). Secondary coatings to hydrophobise materials are often required, although some have shown that hydrophilic polymers can directly form a superhydrophobic surface.[37] Such surfaces have high contact angles but are not usually "slippy" as the fibres penetrate into the water more than halfway and prevent it from spreading purely by being discontinuous. Other work has led to the inclusion of additives in the fibre-spinning process to vary morphology or to add other properties to the fibres. Zhang et al. described the preparation of conductive, magnetic and superhydrophobic carbon nano-fibres, by electrospinning PVA and ferrous acetate.[38] The as-spun fibres were smooth
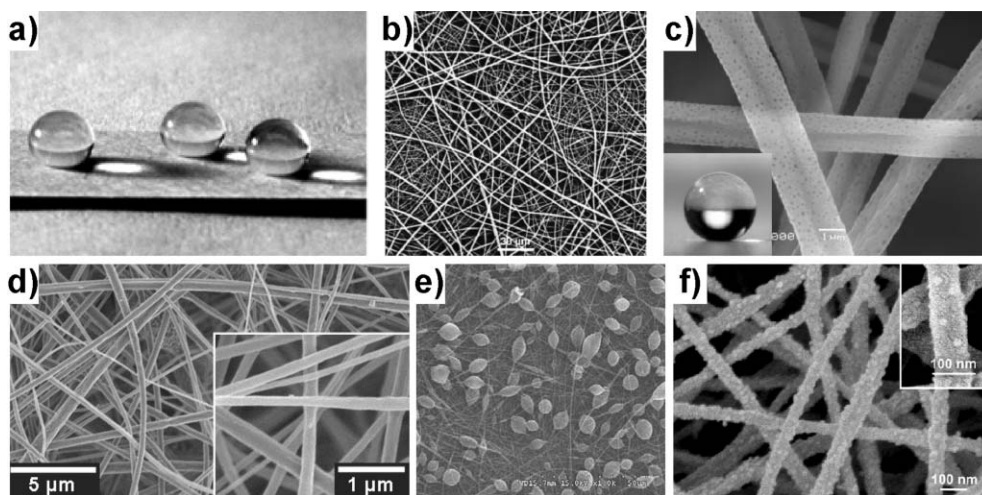

Fig. 4 Superhydrophobic fibre surfaces (a) water droplets on a block copolymer electrospun fibre mat,[23] (b) electrospun fluoropolymer mat,[24] (c) porous electrospun fluorinated fibres,[25] (d) cellulose acetate fibrous membrane,[26] (e) micro-bead connected fibres by electrospinning.[27] Images reprinted with permission from (a) American Chemical Society, Copyright 2005, (b) (c) and (f) Copyright Wiley-VCH Verlag GmbH & Co. KGaA, (d) Institute of Physics, Copyright 2007, and (e) Elsevier, Copyright 2007.

with an average diameter of 180 nm, but after calcination, 20–30 nm diameter Fe_3O_4-filled carbon nano-fibres were formed with ball-like nano-textured surfaces, Fig. 4(f). The WCA on the fibre mats changed dramatically from $\sim 27°$ on the PVA based as-spun fibres to $\sim 157°$ when calcined, due to a change in chemistry and topography of the surface.

Phase separation

Rough surfaces can also be formed by the phase separation of a multi-component mixture. If a stable mixture becomes unstable due to some change, such as cooling, it will begin to separate into two phases, one of which might be a solid or become solid at some point in the process. One of the possible ways that separation can occur is through a bicontinuous structure, Fig. 5(a), where each of the two new phases forms a 3-dimensional network and these networks interpenetrate. The structure is initially very fine, but coarsens over time as interfacial surface area is reduced; the structure eventually collapsing to form two layers (or possibly more if there are more immiscible components). Usually phase separation induced by an environmental change, such as temperature or pressure, may result in remixing if the conditions revert. However, if one component solidifies at the point when a bicontinous structure is formed the second phase may be removed to create a solid 3D porous network. A liquid phase could be removed and the solid does not fall apart because each phase is continuous *i.e.* the solid is a single piece and the liquid can evaporate. The size of the pores in the solid structures formed can be controlled if the rate of phase separation can be altered relative to the rate of solidification. Phase separation is of interest for the generation of superhydrophobic materials due to the low cost and ease of production, and the possibility of creating various shaped substrates by casting and coating.

Bicontinuous structures have been used for many years as filters and chromatography stationary phases. Their use as superhydrophobic surfaces began later with Nakajima *et al.*[44] producing rough films using a sol-gel, this was followed up shortly afterwards by Rao and Kulkarni[45a] and Shirtcliffe *et al.*[45b] Another group cooled polypropylene solutions in solvent mixtures to produce the polymer equivalent.[46] Recent publications in this area have increased the polymers available to include polyvinyl chloride,[41] polycarbonate[47] and polystyrene[48] as well as some fluoropolymers,[43] allowing various surface chemistries and topographies to be investigated, Fig. 5. Many efforts are focused on moving this method towards technical production due to its simplicity compared to most of the others described in this report and the ease in forming a conformal coating. A notable example is the coating of cotton fibres with a sol–gel-derived material.[21] A few researchers diverge from this, highlighting other potential properties[40] or combining the technique with others such as electrospinning[36,49] and micro-contact printing.[50] Block copolymers have also been used, which phase separate internally, often resulting in structured surfaces, which can be deposited from solvents.[42,51]

Phase-separated structures usually have microscale structure; although smaller features are possible these materials are more prone to collapse during drying as the size is reduced. A recent paper describes a method for producing films with small enough structure that they are optically transparent using silica sol–gel and poly(acrylic acid), these films require a coating of a hydrophobic material to render them superhydrophobic.[52] Materials produced generally have features of a single size so WCAs are not always as high as those observed on surfaces with multi-scaled roughness. The transparency and hardness of the materials generally decreases as the structures become larger. Another advantage of having a bicontinuous structure is that it can be cut or abraded to
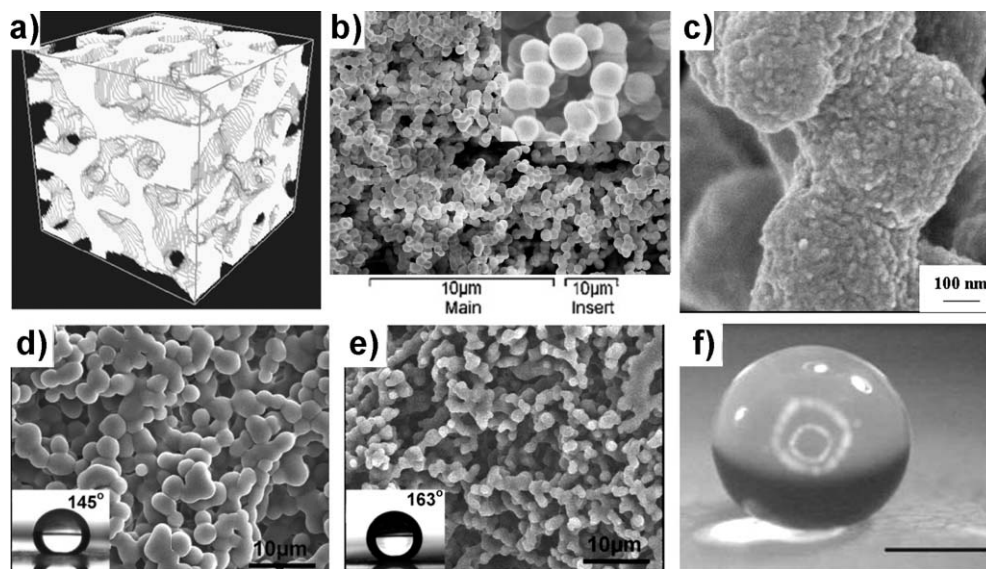
Fig. 5 Examples of phase separation, (a) model of a bicontinuous structure,[39] (b) sol–gel foam produced using acetone as co-solvent,[40] (c) superhydrophobic PVC film,[41] (d) and (e) phase-separated block copolymer films,[42] (f) water droplet on an organic xerogel (scale bar = 1 mm)[43] Images reprinted with permission from (a) American Physical Society, Copyright 2001, (b) and (c) from Elsevier, Copyright 2007 and 2006, respectively, (d) and (e) from American Chemical Society, Copyright 2005, and (f) The Royal Society of Chemistry, Copyright 2006.

reveal a 'fresh' superhydrophobic surface if it becomes contaminated.

Crystal growth

Complex patterns can be generated by crystal growth, from assemblies of simple crystals to fractal snowflakes. During crystallisation various parameters can be altered to influence the size and shape of crystals including the rate of cooling and solvent evaporation or addition. Rough surfaces can be formed on top of a crystallising liquid or by adding a surface to the crystallising system. Superhydrophobic surfaces are then afforded if the material is intrinsically hydrophobic, or a hydrophilic material can be additionally coated.

Crystal growth was first used to prepare superhydrophobic surfaces by Tsujii et al., who controlled the cooling rate of an alkyl ketene dimer (AKD) to form a fractal crystalline surface with a water contact angle of 174°.[58] A recent study found that the AKD surface develops further surface roughness over a few days, increasing WCA to a maximum.[59] Fractal surfaces of wax achieved by natural cooling have also been documented.[4] The formation of a fractal triglyceride surface has recently been reported, having a WCA of 110° upon initial deposition and becoming superhydrophobic as the fractal surface grows.[60] Another recent report in this area makes use of the random crystallisation of n-hexatriacontane, giving water-contact angles as high as 171.8°.[61] Other materials also form rough crystalline surfaces, with one of the simplest routes to a rough superhydrophobic surface reported by Han et al. in 2004.[62] By stretching a thin sheet of poly(tetrafluoroethylene) Teflon® fibrous crystals with a large fraction of void space between them were formed, having a water-contact angle of 165°. Fractal aluminium oxide surfaces have been shown to be super amphiphilic, formed by anodic oxidation and then coated with hydrophobising agents.[63] A recent publication suggested a plasma-enhanced chemical vapour deposition route to form superhydrophobic surfaces of silica and aluminium, which were both hard and transparent, Fig. 6(e).[57]

Amphiphilic inorganic materials

Inorganic materials can also crystallise to form, and some of them are hydrophobic enough to become superhydrophobic when rough. More importantly, many semiconductors are (super)hydrophobic in the dark but become (super)hydrophilic when exposed to light. This property may be attributed to the material being naturally hydrophobic, becoming wetted after the UV-generated creation of free electrons or holes on the material surface. Another explanation is that the materials are in fact hydrophobic due to contamination; which is photo-degraded making the material hydrophilic when exposed to UV (and oxygen).

The first report of an inorganic material demonstrating reversible switching between superhydrophobic and super-hydrophilic states made use of densely packed ZnO nano-rods.[64] However, such ZnO films display superhydrophobicity even if they are sparsely spread over the surface.[65] The low surface energy of the (001) plane at the nano-rod surface combined with the feature size means that high WCAs can be achieved. ZnO surfaces regain their superhydrophobic character after being left in the dark for a few days, although it has been reported that photo-corrosion can be a problem,[66] with ZnO being more unstable in UV light compared to other photocatalytic metal oxides, such as TiO_2, which show the same switchability.[67] Aligned SnO_2 nano-rod surfaces have also been reported for use as superhydrophobic surfaces.[68] These oxide films not only show inherent water-repellent properties that are UV switchable, but are also conductive and 60% transparent in the visible range.

Silver nanostructures prepared via a galvanic cell reaction using $AgNO_3$ and HF have shown superhydrophobic properties after subsequent functionalisation with an akanethiol, Fig. 6(b).[54] These showed high WCAs (154°) with a tilt angle
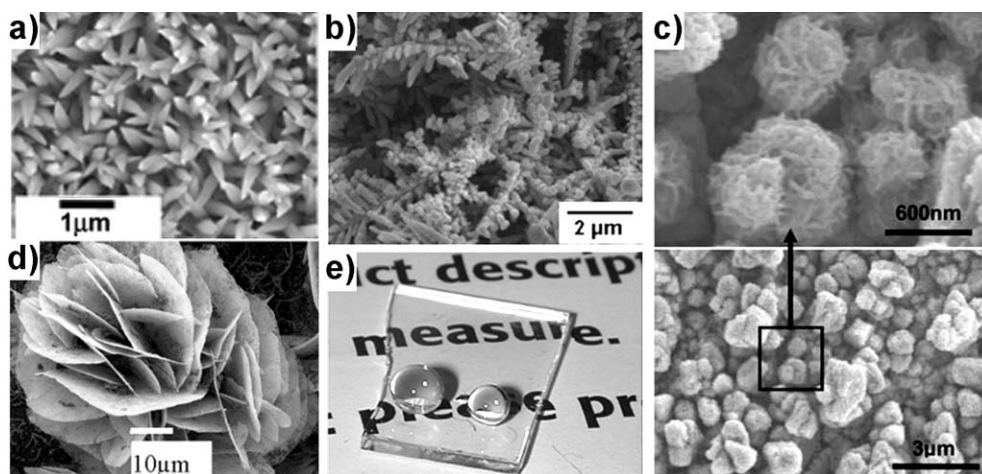

Fig. 6 Rough surfaces by crystal growth (a) cobalt hydroxide crystalline nano-pins (brucite-type) with diameter of 6.5 nm,[53] (b) silver aggregates deposited on a silicon wafer,[54] (c) CuS-coated copper oxide; enlargement shows nanostructure,[55] (d) flower-like tin oxide structure,[56] and (e) transparent superhydrophobic alumina–silica composite film.[57] Images reprinted with permission from (a) and (b) American Chemical Society, Copyright 2005 and 2006, respectively, (c) and (d) The Royal Society of Chemistry, Copyright 2005 and 2004, respectively, and (e) Institute of Physics, Copyright 2007.

lower than 5°. One of the highest water-contact angles achieved so far was reported by Zhou *et al.*, with a water droplet being supported with a contact angle of 178° on a dense array of dodecanoic acid-coated, cobalt hydroxide crystalline nano-pins (brucite-type) with diameter of 6.5 nm, Fig. 6(a).[53] The gas-phase coating of polymethylsilsesquioxane nano-filaments at atmospheric pressure without the need of a carrier gas was described by Seeger *et al.*, achieving inexpensive superhydrophobic surfaces on a variety of substrates.[69] A two-stage preparation of an inorganic surface which mimics the features of a lotus leaf has been carried out, firstly forming micro-globular CuO which is subsequently treated with sulfur gas to produce CuS nano-roughness, Fig. 6(c).[55]

Progression of materials and techniques used to fabricate superhydrophobic surfaces has led to the investigation of other properties that are desirable for many applications: their strength, hardness, rigidity, visible transparency, *etc.* There are many optical applications for superhydrophobic surfaces, which depend on a material being transparent. As the scale of surface roughness is increased the scattering of light also increases, therefore diminishing the transparency of a material. Since visible light is in the range 350–750 nm a surface would have to have features less than 100 nm to be completely transparent to visible light. Nano-rod arrays are of particular interest because superhydrophobic surfaces generated from them are highly resistant to pressure, have extremely high specific surface areas and can be transparent to optical wavelengths. They can also often be applied conformally to complex shapes. There are a few mechanisms for the growth of these materials.

Nanostructured crystals

Crystal growth. The simplest mechanism is where conditions are arranged so that the crystal face parallel to the surface grows fastest. If distributed nuclei are present, or formed on the surface, this leads to the growth of pillars. This most commonly occurs in oxides of metals, such as zinc and cobalt. Deposition can occur from dissolved species or from the gas phase, but the window of conditions allowing organised growth is often small. Nano-columns can also grow from screw dislocations. Usually a lattice misfit between the adlayer and the substrate gives rise to distributed dislocations, which then grow in spirals to form cones. The screw dislocation is usually visible in the centre of the column.

Zinc oxide crystals can grow to form arrays of oriented nano-columns either by vapour deposition or from a solution phase; these show a high degree of hydrophobicity when hydrophobised[70] Recently, nanostructured films of WSe_2 and MoO_3/MoO_2[71] have been reported and, although these only have a water-contact angle of 125°, the ability to tune the film structure during vapour deposition could lead to a range of surface wettabilities upon further chemical modification. SnO_2 'nano-flowers' have also been grown and demonstrated to have superhydrophobic character, Fig. 6(d).[56] These were prepared *via* thermal oxidation of a tin organometallic precursor. Nanostructured flower-like crystals can also be prepared by the controlled crystallisation of polyethylene from xylene by the addition of a non-solvent (cyclohexanone).[72]

Catalysed growth. Nano-columns can also be formed using a sputtered array of metal particles to control the growth. Usually gas-phase reagents condense on the catalyst particles and form a solid or liquid solution. Eventually a fibre or tube starts to grow from each particle, either on top of the particle or below it, lifting the particle as it grows. Once this type of growth begins it can generate structures with very high aspect ratio. Carbon fibres can be grown in this manner using transition-metal catalysts, but silicon oxide and other materials have also been generated. Usually growth takes place at high temperatures as diffusion through the metal must occur. Carbon nanotube arrays are the most popular of these surfaces. Such films are often termed 'nanograss' or 'nano-forests' and can be chemically modified to present a rough and hydrophobic surface. The first report by Gleason *et al.* described how a water droplet could be supported almost as a sphere on PTFE-coated nanograss.[73] Other coatings, such as thiol SAMs and ZnO, have been used, the latter having the advantage of being switchable from superhydrophobic to superhydrophilic as discussed above.[74] More recently, carbon-nanotube coatings have been applied as a secondary coating on top of micro-machined posts to give 2-tier roughness – mimicking the lotus leaf.[75] A general review of the wetting properties of carbon-nanotube films has been given by Liu and Jiang.[76]

Porous aluminium oxide

Aluminium oxide layers can be grown on aluminium metal under anodic potentials in acid. The oxide forms nano-pores in a hexagonal array with sizes determined by the potential used. The growth of the structure is determined by the size mismatch between aluminium oxide and the underlying metal as well as electrostatic repulsion between the pore walls mediated by the electric potential. The porous arrays have been used to template aligned nano-columns of various materials including carbon, polymers and metals. Polystyrene nanotubes formed in this way show high water-contact angles but also cause droplets to stick to their surface.[77] Titanium oxide also forms similar patterns and can be used to generate superhydrophobic surfaces when coated.[78]

Differential etching

Although etching can polish surfaces it generally increases the roughness of the substrate. This is often due to differences in the relative rates of etching of different crystal planes or of the matrix compared to crystalline regions. Roughness is generated on the order of the crystallite size or smaller, depending on the method used. This mechanism can be used to generate suitably rough surfaces to cause superhydrophobicity, either straight away or after treatment with a hydrophobising agent, depending on the substrate used.

Early etching methods utilised plasma and ion etching or laser ablation of polymers, initially PTFE,[83] but other polymers are also suitable such as polypropylene.[1b] This results in considerably roughened surfaces and can be carried out on a relatively large scale. It is often necessary to add a monomer to the gas phase during plasma etching to repair any

hydrophilic damage that occurs. Later, wet etching of metals was investigated, allowing many materials to be made super-hydrophobic with relative ease.

Ion etching followed by oxygen glow-discharge was used to roughen FEP-Teflon forming a superhydrophobic surface, achieving WCAs up to 150°.[84] Higher WCAs have been achieved by argon plasma etching polypropylene in the presence of poly(tetrafluoroethylene).[1b] Nanostructured poly(ethylene terephthalate) has been prepared by domain-selective oxygen plasma etching, a technique which does not require high temperatures and so can be used for the preparation of roughened surfaces using a variety of polymeric materials.[85] Oxygen plasma etching has also been used to prepare optically transparent poly(ethylene naphthalate) and polystyrene, forming nanostructures which were then treated with organosilanes to produce superhydrophobic surfaces.[86] More recently, oxygen plasma processing has been used to produce transparent poly(methyl methacrylate) surfaces, which can be treated with a fluorocarbon to afford superhydrophobic character.[87] The advantage of this reported technique is the speed of the method, with a total processing time of a few minutes, and the large size of samples – depending on the size of the plasma chamber used.

In 2000, the investigation of superhydrophobic surfaces for the reduction of ice-crystal formation steered Narita et al. to prepare nano-pitted aluminium.[88] Large pits were formed by electrolytic etching followed by smaller pits introduced by anodic oxidation. After functionalisation with a fluoroalkylsilane the surfaces showed superhydrophobic character. Aluminium, zinc and copper are polycrystalline metals which have been used to form superhydrophobic surfaces by wet chemical etching. These substrates were etched by a dislocation etchant, preferentially dissolving the dislocation sites in the metal grains to give a rough surface.[89] Copper etching was also used by Shirtcliffe et al. to produce multi-scale roughness.[8]

Aluminium alloy has been used more recently to form surfaces with micro-protrusions and nano-particles, with an additional spun-coated layer of either perfluorononane or vinyl-terminated poly(dimethysiloxane) to give superhydrophobic surfaces, Fig. 7.[79]

Recent developments using etching to engineer materials have widened the range of metals used to include titanium materials.[90] The TiO$_2$ layer was etched using a RF plasma using CF$_4$ as etchant. The rough surfaces were then chemically modified to give high WCA and low hysteresis surfaces. Qu et al. have suggested a nitric acid and hydrogen peroxide wet chemical etch solution for the treatment of steel and copper alloys, and hydrofluoric acid/hydrogen peroxide for titanium alloys.[91] Silicon can also be roughened using ethanolic hydrofluoric acid and anodic etching.[92] This is a two-stage process wherein small pores are formed first, then an additional wet etching step modifies the porous layer to a pillared structure. The crystallisation of metal alloys can also be controlled to produce rod-like crystals that can be revealed by selective etching of the eutectic; etching time determining the height of the features exposed.[93] A femtosecond laser has also been used to create micro/nanoscale roughness on a silicon wafer, with the laser fluence being varied to control the induced morphology, Fig. 7(b) and (c).[80] Another way to achieve 2-tier roughness of silicon was reported by Kim et al., using a combination of CF$_4$ glow-discharge etching and masking with copper nano-dots.[94] These surfaces were treated with hexamethyldisiloxane to give high WCAs and low hysteresis.

An article examining the adhesive properties of nanostructured surfaces – mimicking gecko foot hair also uses a deposited metallised mask to form nano-features.[95] Aluminium discs were formed on a polyimide film by a standard lift-off technique; they were then used as a surface mask during plasma etching.
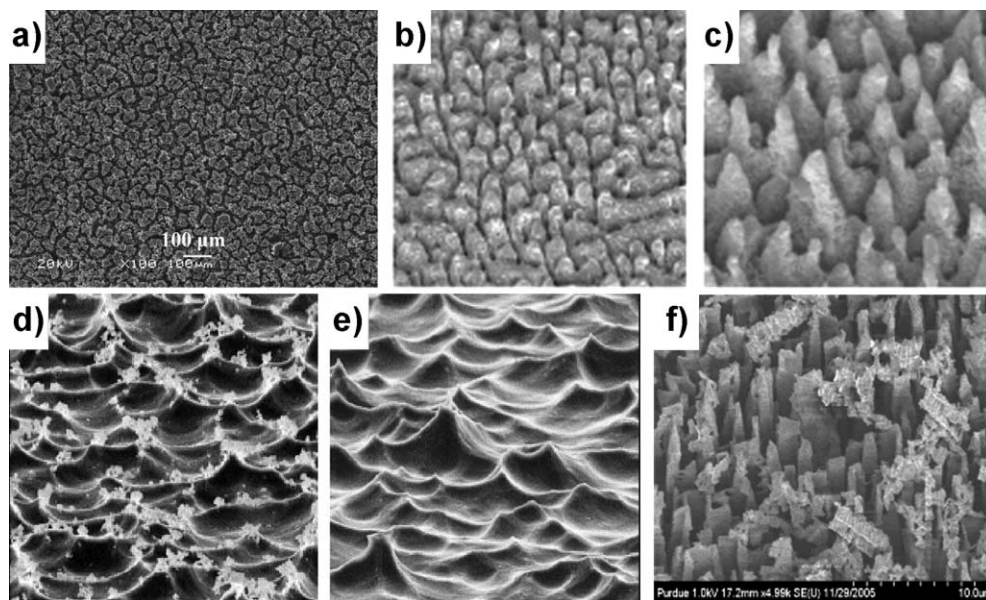

Fig. 7 Etching (a) roughened aluminium alloy,[79] (b) laser-etched silicon surface in SF$_6$ 3.2 kJ m^{-2} and (c) using 5 kJ m^{-2},[80] (d) silicon wafer/photoresist layer over-etched by an inductively-coupled SF$_6$ plasma before cleaning,[81] and (e) after ultrasonication to remove residual photoresist, and (f) submicron pillar structures in p-type silicon after buffered oxide etching.[82] Images reprinted with permission from (a), (d) and (e) Elsevier, Copyright 2006 and 2005, and (b), (c) and (f) American Chemical Society, Copyright 2006 and 2007.

Diffusion-limited growth processes

The formation of roughness during deposition of layers of material is common and is often considered to be an unwanted side effect. Generally some species, either in solution or in gas phase, approach the surface and adsorb; they may later move around on the surface, bond permanently or desorb. Rough surfaces are most efficiently formed when the approaching species bond instantly to the surface, which means that the concentration of unbound species at the surface is effectively zero and the rate of deposition is only dependent upon the flux of material – diffusion-controlled deposition. Initially this has little effect upon the surface morphology, but any protruberation gathers more material than the surrounding area. Growth is concentrated at these points so when any roughness is generated by chance it increases rapidly. As the structures get larger the same effect occurs on their sides, generating a branching structure with some fractal character. This roughness growth can occur during electrodeposition and gas-phase deposition. The appearance of such surfaces and their branching characteristics depend upon the growth process, but they usually resemble cauliflower florets, Fig. 8.

Early research was carried out using plasma-deposited polymers. The superhydrophobicity of these surfaces was recognised around 1997.[99,100] Fluorocarbons were often used, but silanes were also popular.[99] The method showed early promise, as plasma-deposited polymers are relatively hard and the process is often used to deposit technical coatings on high value or small components. Research publication on these has slowed as the technique has matured.

Electrodeposition is more accessible to most research departments and allows the formation of similar fractal structures if conditions are set so that the deposition is diffusion limited.[101] These must usually be coated with a thin layer of hydrophobising agent to make them superhydrophobic, so were not investigated until somewhat later. Initially metals and metal oxides were used, with zinc oxide being used in 2003,[102] being joined by copper,[8] gold[103] then titania[97] in 2005. Conducting polymers have also been used, many of these have the useful property of being switchable from conducting and hydrophilic to non-conducting and hydrophobic.[104]

The surfaces, being fractal, are usually very highly hydrophobic, some of them are quite strong, but most are easily damaged and few are transparent as the fractal patterns have structures on many length scales.

Most of the more recent publications concentrate on methods more suitable for industrial realisation as most basic research has been covered. One report highlights the ability to transform a cheap polymer film into a transparent superhydrophobic film with a plasma polymer by ensuring that the roughness scale remains small.[105] Other plasma techniques being used are cheaper and cover larger areas, including expanding arc plasma using a low vacuum and completely atmospheric pressure techniques.[96,106] Although the methods are different the properties of the films and their structures are similar to those initially studied. Electrochemical techniques using electroless deposition also show greater suitability to industrial application.[107] The early reported are still referred to in papers, often as standard superhydrophobic surfaces.[108]

Also apparent is a general move towards generating nanoscale roughness. An example is silver nanostructures prepared *via* galvanic replacement,[54] which showed high water-contact angles and low hysteresis after hydrophobisation. Others add different techniques together to produce more complex surfaces, such as an example using electroless deposition onto areas of a surface selected by chemical
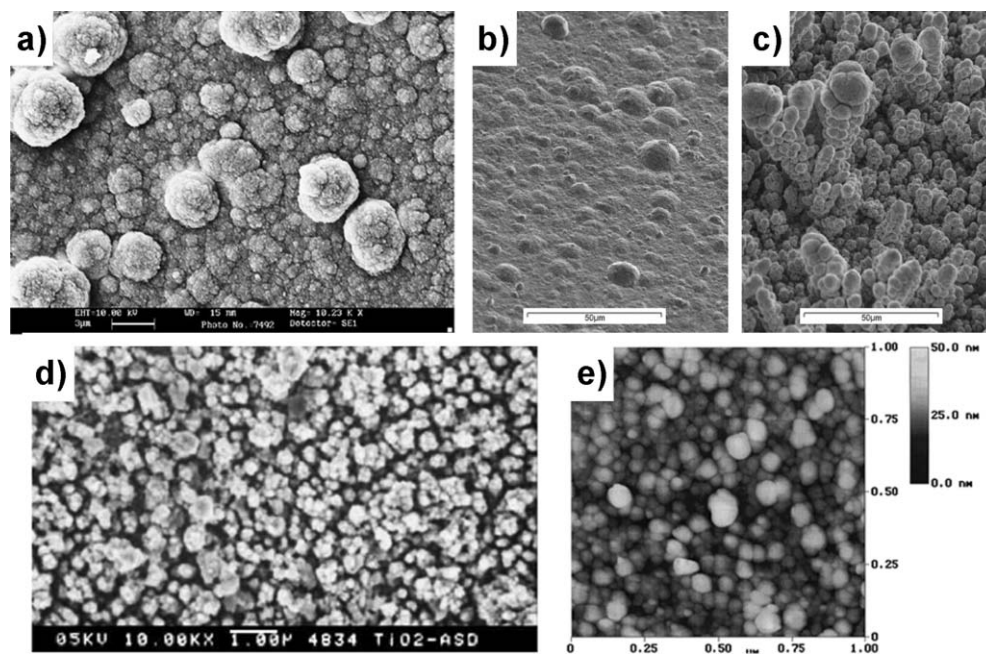

Fig. 8 Diffusion-limited growth on surfaces (a) plasma-deposited Teflon structures,[96] (b) electrochemically deposited copper at 100 mA cm^{-2}, and (c) 200 Ma cm^{-2},[8] (d) an electrodeposited amorphous TiO$_2$ thin film,[97] and (e) HMDS plasma-deposited polymer.[98] Images reprinted with permission from (a), (d) and (e) Elsevier, Copyright 2007, 2005 and 2001, respectively, and (b) and (c) American Chemical Society, Copyright 2005.

patterning.[109] The combination of diffusion limited growth and etching has been reported for the production of a nano-needle array[110] Another example is a growth pattern of an organic salt where crystalline structures are affected by diffusion limitations, growing an extremely rough surface.[111]

Plasma polymers are also used as thin hydrophobising coatings on other roughened surfaces, it is often unclear how smooth these layers are by themselves, although it is possible to generate very smooth layers using this technique.[112,113]

Lithographic techniques

Lithography encompasses many different types of surface preparation in which a design is transferred from a master onto a substrate surface, allowing multiple copies to be made. Methods closest to the original meaning of the term involve contact between an inked stamp and the substrate, with micrometre-sized features being standard and the newly established nano-imprint lithography (NIL) allowing smaller patterns to be produced. In photolithography a photoactive polymer layer is irradiated through a mask followed by developing stages where either the exposed or unexposed polymer is removed, leaving a positive or negative image of the mask on the surface. Photolithography can de sub-divided into different categories depending on the radiation used: UV, X-ray, e-beam, etc. It is also possible to use a laser or particle beam to etch the surface directly or to expose a photoresist layer, but this is relatively slow. The patterned surface is then either used as is, or used as a mask on the substrate for deposition or etching. Lithography is useful for generating superhydrophobic surfaces where the shape of the features and the pattern is well-defined. For this reason it has mostly been employed to generate surfaces allowing theories of super-hydrophobicity to be tested, although more recently direct applications have been suggested. Lithographic processes are often used to produce master surfaces, for instance in photoresist, which are then used as templates for the casting of the desired surface features in another material. These types of lithographic templating are covered in a later section.

One of the first reports using photolithography to produce 3D surface features for the investigation of wetting was by Kawai and Nagata in 1994,[120] although these features were of low aspect ratio (height/width) they did show a change in wett-ability with respect to feature height. Oner and McCarthy[114] produced a larger range of feature sizes with patterns etched in silicon, including square posts from 20–140 μm height and side lengths 2–128 μm, Fig. 9(a) as well as staggered rhombus- and star-shaped structures, Fig. 9(b). A similar silicon-processing technique was reported by Zhu et al.,[116] giving square pillars in the range 10–85 μm, Fig. 9(d), and more recently by Dorrer and Ruhe[121] to generate smaller posts. Shirtcliffe et al.[8] reported a technique using patterns in SU-8 photoresist. Circular pillars were produced with diameters from 2 to 40 μm and up to 80 μm in height Fig. 9(g). Similar surfaces were used in a later study to assess electrowetting on model super-hydrophobic surfaces.[122] SU-8 features have been investigated further by Suzuki et al. who looked at the wetting of hexamethyldisiloxane plasma-coated features with various size
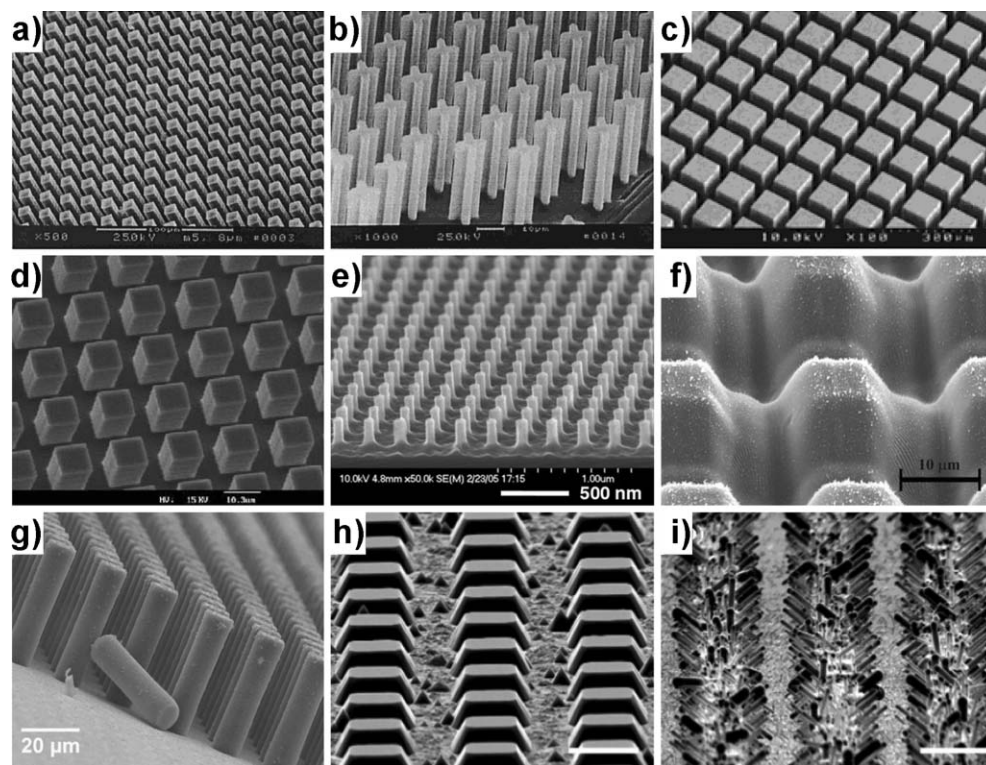

Fig. 9 Lithographic surface modification (a) photolithographic towers and (b) indented square posts,[114] (c) diced silicon wafer,[115] (d) photolithographic towers,[116] (e) silicon nano-towers,[117] (f) laser-modified SU8 surface,[118] (g) SU8 towers,[8b] (h) silicon islands and (i) silicon nano-wires grown on those silicon islands.[119] Images reprinted with permission from (a), (b), (c), (f), (h) and (i) American Chemical Society, Copyright 2000, 2002, 2006 and 2007, (d) Elsevier, Copyright 2006, and (e) and (g) Institute of Physics, Copyright 2006 and 2004, respectively.

and shape as well as inter-pillar spacing.[113] Wagterveld et al.[118] used high-energy excimer laser pulses to create microstructures in SU-8 by photochemical laser ablation and, as a side effect of the ablation process, nanoscale roughness was introduced as a result of the generation of debris, Fig. 9(f). Water-contact angles on these surfaces coated with a hexafluoropropene layer were measured at 165°. SU-8 has also recently been used to produce patterned micro-arrays with hydrophilic areas surrounded by superhydrophobic zones.[123]

An alternative technique used by Yoshimitsu et al.[115] in 2002 employed a mechanical dicing saw to produce stripes and square pillar structures in silicon wafers, Fig. 9(c). Feature sizes as small as 50 μm were achieved although smaller features would be very difficult to prepare using this technique. Electron-beam etching, however, has been successfully used to direct write pits and pillar structures into silicon.[124] The height/depths were in the range of 116–792 nm and the diameters 105–157 nm. Investigation into the shape and curvature of the feature edges suggested that these play an important role in determining advancing WCAs. Silicon-pillared structures 1–4 μm tall with 1–2 μm diameters were prepared using X-ray lithography by Furstner et al.[125] This article is particularly relevant when considering biologically inspired superhydrophobic surfaces as lithographically prepared surfaces are compared to microstructured copper and aluminium foils and replicates of Alocasia, Rosa and Nelumbo leaves. More recently, the impressive fabrication of a dense array of nano-sized silicon structures has been reported over a large sample area (4 cm^{-2}).[117] Here a combination of deep reactive ion etching and interference (holographic) lithography was used to produce pillar structures in silicon with feature size of the order of tens of nanometres, with the tips of these features being further 'sharpened' by thermal oxidation and removal of the oxide, Fig. 9(e). Cao et al.[119] reported a silicon-processing technique using a combination of photolithographic patterning and various etches. Subsequent growth of silicon nano-wires via chemical vapour deposition afforded hierarchical roughness, allowing samples to be produced having overhang structures, Fig. 9(h) and (i). These surfaces were superhydrophobic to water droplets even though the intrinsic contact angle of the silicon is only 74° (as were those of Shirtcliffe et al.[8] in SU-8 with a WCA of 81°). Upon immersion into water the wetting mode switches from Cassie–Baxter to Wenzel and the surfaces become fully wetted, a cycle that could be repeated after the sample was dried.

A nano-imprint lithographic process has been used to fabricate an ordered array of grooves into a silicon substrate, by first imprinting a photoresist layer with a stamp followed by ozone treatment and wet etching.[126] Water-contact angles as high as 167° were measured on these surfaces after treatment with octadecyltrichlorosilane. Recently, nano-imprinting has been used for the production of replica plant leaves, with a nickel relief being electroformed around the original. After dissolution of the leaf, the stamp was then used to create replica leaf-type structures in photoresist by UV-NIL with WCAs being measures as high as 168°.[127]

From the first report in 1994, lithographic techniques have been developed to reduce feature sizes and yield larger structured areas. The potential for industrial applications requires surfaces to be processed rapidly and to be reproducible and cheap.

Aggregation/assembly of particles

Colloidal particles can form close-packed assemblies on surfaces by either spin-coating, dip-coating or reverse-dip-coating methods. By utilising the attractive Van der Waals forces between particles a tightly packed layer (if a mono-disperse colloid is used) can be formed, introducing ordered roughness on the order of the particle size used. Electrostatic repulsion can be exploited to generate films of spaced particles, although these are generally less ordered. This method is comparatively low cost, can be applied to fairly large surface areas and does not require any specialised equipment. The arrays of particles are also photonic crystals and therefore display useful and attractive optical properties.

Silica particles are often used to form hexagonally close packed arrays with particle sizes ranging from a few nanometres to a few hundred micrometres. Such arrays can be functionalised by silanes to produce superhydrophobic surfaces.[130] Here advancing WCAs were measured at 150°, the angle was not dependent on the silica particle size.

Polymer spheres can also be used to make ordered superhydrophobic surfaces[131] with a recent article describing the use of functionalised silica/latex particle suspensions as superhydrophobic coatings.[132] Aggregated particle surfaces with tuneable wettability have also been demonstrated, using a poly(styrene-n-butyl acrylate–acrylic acid) polymer-sphere array.[133] Here the wettability of the material is affected by surface segregation of the polymers (n-butyl acrylate–styrene ratio), allowing surfaces to have tailored hydrophobicity. Another colloidal crystal, fabricated from polystyrene-block-poly(methyl methacrylate)-block-poly(acrylic acid) was reported to have similar characteristics.[134]

The superhydrophobicity of these arrays can be increased by adding a second layer of roughness to the particles, this has been achieved in several ways including; aggregating different sized particles together to produce "raspberries";[135] sputtering gold on top and heating to form gold nano-clusters, giving higher contact angles of 160°;[136] one of the most recent articles on this subject details the use of a colloidal array of polystyrene beads coated with carbon nanotubes, Fig. 10(b).[128]

More random arrays of particles are also useful for creating superhydrophobic surfaces and also often give rise to higher contact angles than organised structures. A recent article describes the grafting of pH and temperature-sensitive amphiphilic block copolymer brushes to silica spheres to produce switchable surfaces.[137] Particle aggregation was then controlled with solution acidity forming a range of surfaces having different aggregate density. Heating above the coating polymer's glass transition temperature or treatment in acidic water was shown to switch the surfaces between super-hydrophobic and hydrophilic. Another approach was reported by Wang et al., adhering sparsely packed CaCO$_3$-loaded hydrogel spheres onto a surface to act as a template for later adsorption (and aggregation) of silica or polystyrene spheres.[138] The template spheres act by displaying a markedly different hydrophilicity compared to the bare substrate, thus
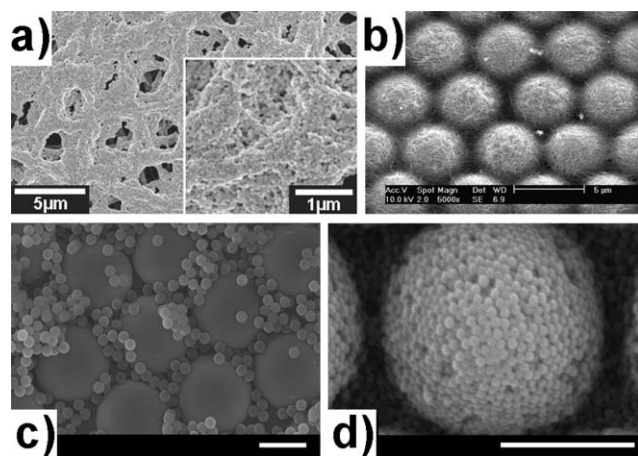
Fig. 10 Particle aggregation (a) layer-by-layer deposition of TiO$_2$ particles on fibres,[26] (b) CNT-coated polystyrene-sphere array,[128] (c) silica-sphere array with additional smaller sphere aggregates (scale bar = 5 μm) and (d) micron-sphere array produced from 300 nm particles silica nano-spheres (scale bar = 5 μm).[129] Images reprinted with permission from (a) Institute of Physics, Copyright 2007, (b) American Chemical Society, Copyright 2007, (c) and (d) Elsevier, Copyright 2007.

subsequent adhesion of polystyrene or silica spheres occurs only on the bare substrate. The resulting hierarchical roughness was then gold-coated and thiol-functionalised to afford a superhydrophobic surface.

The attraction between electrostatically charged species is often used to build up multi-layer structures by sequential dipping in positive and negative polyelectrolytes – a method termed layer-by-layer assembly. A simple layer-by-layer structure using only polymers: polyallylamine hydrochloride (PAH) and poly(acrylic acid) (PAA) have been shown to afford a rough micro-porous structure after acid treatment, which was subsequently coated with silica nano-particles and further silylated to form a superhydrophobic surface.[139] Layer-by-layer assembly can also be used to control of the arrangement and aggregation of particles on a surface, using alternating polymer and charged particle layers, Fig. 10(c).[129,140] Surfaces with gradients from superhydrophilicity to superhydrophobicity have been prepared by graded UV exposure of such layer-by-layer deposited structures.[141] TiO$_2$ particles have also been aggregated around cellulose fibres using PAA to achieve a WCA of 162° after modification with a fluorosilane, Fig. 10(a).[26] Shiratori et al. give a concise overview of the recent developments of polyelectrolyte multi-layer fabrication.[142]

Particle aggregation can be used to form surfaces with ordered or non-ordered roughness on scales from nanometres to micrometres. The advantage of this method is that the particle coating is conformal and readily controlled. Recent developments in this field have seen particle assemblies being produced in the shape of larger structures, Fig. 10(d),[129] with several patents on this type of technology being granted.

Templating

A pattern or shape, either 2D or 3D, can be replicated using a templating method, wherein a material is printed, pressed or grown against the voids of a template. Often the template is then removed, leaving the inverse of its pattern; this can be used as a template to achieve a replica of the original. Templating surfaces is often fast, very low cost and reproducible and so is a widely used method for the preparation of polymeric surfaces. Any surface can be used as a template, such as colloidal, lithographic and woven material surfaces, some of these masters maybe reused and some may be intentionally destroyed to reveal the replica surface. If ordered structures are required with small length scales, lithography of some sort is often used to realise the master templates.

In 1999, Bico et al. produced a master surface via photolithography having features in the micron range.[143] The spikes, shallow cavities and stripes of the master were then replicated using an elastomeric mould, which was subsequently used to cast silica features onto a silicon wafer, Fig. 11(a). Following a hydrophobic self-assembled monolayer coating, the spikes gave an advancing contact angle of 170° compared to 118° for the unstructured surface. Zhu et al. later described the use of a template-based extrusion method for the preparation of much smaller structures via templating.[148] An anodic aluminium oxide (AAO) membrane was used as the template to produce a poly(vinyl alcohol) aligned nano-fibre surface. As with some of the lithographic surfaces, this produced a superhydrophobic surface with slightly hydrophilic chemistry. Similarly an AAO template was used to for perfluoropolyether derivative nano-pillars having superhydrophobic character, Fig. 11(f).[147] Porous aluminium oxide has also been used as a nano-imprint template, pressed into heated polystyrene substrates and removed by dissolution of the aluminium oxide to produce large area polystyrene nano-pillars or nanotubes.[149] Another approach to template-based surfaces is to build the negative master directly. He et al. described the use of PDMS template surfaces produced from a micro-machined master having fairly large micron-sized features.[150] These surfaces were used to investigate the effects of surface structure on wetting; looking particularly how transition from Cassie–Baxter to Wenzel states occurs.

More recently, replicas of superhydrophobic surfaces such as a lotus leaf have been used with amazing success. Sun et al. cast a lotus leaf in PDMS to form a master template then used this to produce a PDMS replica.[151] The randomly arranged micron-sized surface protrusions as well as the nanoscale architecture created by wax crystalloids on the original lotus leaf were clearly copied, with both surfaces exhibiting superhydrophobicity and an advancing WCA of 160°. Indeed there is much interest in natural superhydrophobic surfaces, with researchers focusing mainly on leaf structures.[152] Lee et al. have investigated the feasibility of producing superhydrophobic surfaces by templating the micro/nano surface features of various leaves: tulip tree, silver maple, bamboo and lovegrass.[153] Here an inverse of the leaf structure was fabricated in a photoreactive polymer via nano-imprint lithography, and although a direct replica of the original structure was not achieved the surfaces were superhydrophobic. A progression of this work to produce direct replica of various leaves was reported recently by Suh et al., who cast a PDMS negative and then used this to create a moulded PDMS positive of lotus and
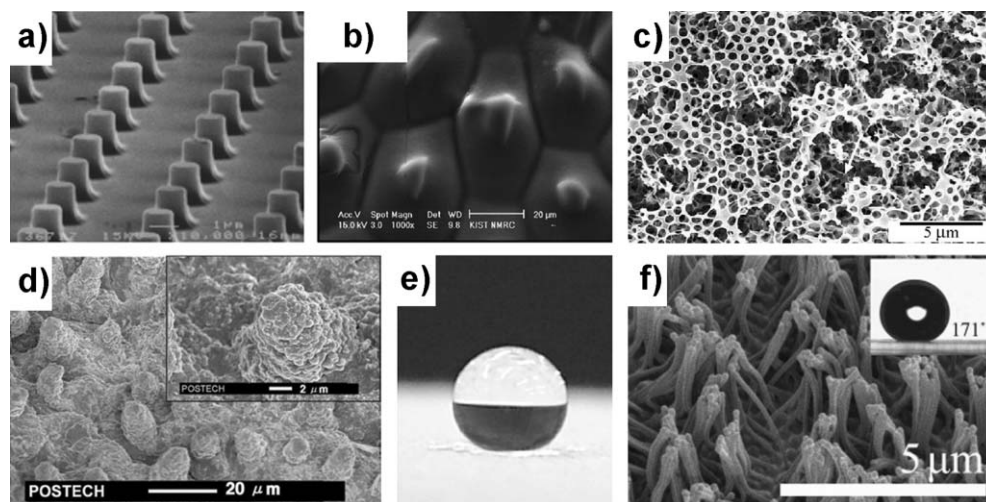
Fig. 11 Replica surfaces produced by templating (a) micro-posts,[143] (b) PMMA replica of *Colocasia*-like leaf surface,[144] (c) a polyvinylidene fluoride inverse opaline structure,[145] (d) photoresist replica of lotus leaf by UV-NIL,[127] (e) water droplet resting on a polymer hot-press transferred pattern,[146] and (f) polymer hairs grown through an AAO template with insert showing water droplet resting on surface.[147] Images reprinted with permission from (a) EDP sciences, Copyright 1999, (b) and (c) Elsevier, Copyright 2007 and 2006, respectively, (d) Institute of Physics, Copyright 2007, and (e) and (f) American Chemical Society, Copyright 2006.

Colocasia leaves, Fig. 11(b).[144] These methods have shown excellent reproducibility of the original template leaves, although the longevity of the PDMS negatives is questionable. A metallised negative replicate of a lotus leaf has been reported that has obvious advantages for mass production, Fig. 11(d).[127] Here nickel was electroformed around a gold-coated leaf to afford a nickel mould.

One of the first reported uses of sacrificial templates to generate superhydrophobic surfaces was by Whitesides *et al.*, who fabricated sub-micron half-shell features by depositing metals onto a silica-colloidal array.[154] After dissolution of the template the nanometre-thick metal cups were aggregated on surfaces and treated with alkanethiols to afford superhydrophobic surfaces. A similar approach using a close-packed silica-sphere array as a template was adopted more recently, wherein gold was electrodeposited between the spheres.[155] Removal of the template led to an hexagonal array of partial spherical pores, with the surface showing superhydrophobicity. This technique has also been used by Jia *et al.*, who used a monolayer of close-packed polystyrene particles as a template and filled the gaps between the particles with silica *via* a sol–gel route.[156] The template was dissolved leaving an inverse hemispherical array. This method is very useful to prepare dual scale features. Similarly fluoropolymeric films have been templated around a silica-sphere array, dissolving the spheres to give a macroporous solid, Fig. 11(c).[145] A recent article has shown how a surface with ordered multi-scale roughness can be created by templating a colloidal array.[129] The paper describes two routes, the first coating an array of micron-sized silica spheres with nano-sized spheres, and the second templating an array of micron-sized spheres in PDMS, which is then used as a mould to produce a crystalline solid of nano-sized spheres, Fig. 10(d). A similar result was obtained by sandwiching an aggregated polymer-beaded surface against a crimped stamp, giving dual scale roughness and a WCA of 160°, Fig. 11(e).[146]

Multiple scale roughness

An issue that has returned to recent discussion is the effect of multiple scales of roughness. The original biological surfaces were often found to have roughness structures on several scales, typically with features of several micrometres with nanometre-sized roughness too, Fig 2.[10] This was investigated previously theoretically[157] and experimentally.[158] More recent theoretical contributions support the earlier suggestions that multiple layers of roughness enhance several aspects of superhydrophobicity; the ease that drops roll off surfaces;[159] the tendency for impacting drops to remove contamination[160] and the prevention of conversion between Cassie–Baxter and Wenzel states of wetting.[161] Experimental evidence suggests that surfaces with sufficient multiple roughnesses can condense water in the Wenzel state and then convert to Cassie–Baxter, allowing the drops to run off easily.[75]

Recently there has been a general trend towards producing surfaces with multiple scale roughness. These can be achieved with single techniques, such as diffusion-controlled electrochemical deposition.[162] Often, however, several steps or methods are combined, giving rise to: growth of crystals during etching;[163] assembly of colloidal particles with a second layer of roughness on top by adding another layer of smaller particles[128] or by crystallisation on the particles;[136] combining templating and particle arrays[129,156] or particle arrays and lithography;[146] a combination of templating and etching also provides dual-scale roughness.[94]

Outlook

Superhydrophobicity is a fairly recent term used to describe the extreme water repellency of rough hydrophobic surfaces; however, the science has been around for much longer. Hydrophobic fabrics, ultrahydrophobic surfaces, water-resistant materials and superhydrophobicity are among the

most used terms, although the exact meaning of each is rather vague, particularly when describing hysteresis character. We have suggested standardising terms in the introduction. Early products include breathable fabrics and some membrane filters, which use the plastron effect of superhydrophobic surfaces,[164] but these are rarely referred to as being super-hydrophobic as their use predates the term (*e.g.* Gore-Tex patented in 1972®).[165] A recent paper by Gao and McCarthy highlights this by showing that a technique designed in 1945 produces superhydrophobic fabrics,[19] the term superhydro-phobicity arose around 1991.

The number and scope of techniques to generate super-hydrophobic surfaces has greatly increased in recent years with suggested applications expanding with them. The main barrier preventing self-cleaning surfaces being used in many areas is that the surfaces are easily damaged or contaminated during normal use, such as abrasive wear and washing cycles. Despite this over 200 patents have been granted that use or produce superhydrophobicity in some form and products are becoming commercially available. Some applications do not involve abrasion or contact with oils that may cause contamination, and have made use of these super-water-repellent surfaces. Communication and radar antennae and receivers are some-times coated with superhydrophobic paint to reduce water/ice-induced distortion (*e.g.* Hirec by NTT-AT corp. Japan). STO corp. (USA) is a manufacturer of high-quality building materials which has been marketing an exterior paint since 1999 under the trade name Lotusan®, an apparently successful product. Other general coatings are available from Degussa GmbH (Germany) and some further recent products are more resistant to scratching and are, or will be, applied to LCD screens and CDs to protect them, being produced by TDK and Sony (Japan). As research continues, methods of production and materials used to form superhydrophobic surfaces broaden, opening new avenues for potential applications. A recent report highlights the possibilities for superhydrophobic surfaces to reduce bio-adhesion, which is a problem in a huge range of areas.[166]

One would imagine that superhydrophobic surfaces would be useful on glass surfaces to keep them clear of condensation and water drops. Although the dew point is reduced on superhydrophobic surfaces condensation still occurs if the temperature difference and humidity are great enough. Raindrops rolling off a superhydrophobic glass surface, or even a hydrophobic one, can be more distracting than if the surface is hydrophilic. For this reason most coatings for windows and mirrors are superhydrophilic, causing condensa-tion and drops of water to form a film, which is not easily visible when viewed perpendicularly (*e.g.* products by Ventree Co., Korea). Superhydrophilic surfaces, particularly those with photo-oxidative properties, are also being used as coatings for roof tiles (*e.g.* products by Erlus AG, Germany, and by Deutsche Steinzeug Cremer & Breuer AG, Germany) and in paints (*e.g.* Japan Hydrotech Coatings Co., Japan). This area is well-established with coatings continually being developed and improved, although it should not be confused with those displaying superhydrophobicity.

As coatings improve and prices fall the use of super-hydrophobic surfaces is likely to increase, particularly as many of the drawbacks are now well-understood and some can be minimised by choosing specific coatings.

References

1 (*a*) R. Blossey, *Nat. Mater.*, 2003, **2**, 301–306; (*b*) W. Chen, A. Y. Fadeev, M. C. Hsieh, D. Oner, J. Youngblood and T. J. McCarthy, *Langmuir*, 1999, **15**, 3395–3399; (*c*) M. Callies and D. Quere, *Soft Matter*, 2005, **1**, 55–61; (*d*) L. Feng, S. H. Li, Y. S. Li, H. J. Li, L. J. Zhang, J. Zhai, Y. L. Song, B. Q. Liu, L. Jiang and D. B. Zhu, *Adv. Mater.*, 2002, **14**, 1857–1860; (*e*) T. L. Sun, L. Feng, X. Gao and L. Jiang, *Acc. Chem. Res.*, 2005, **38**, 644–652; (*f*) X. J. Feng and L. Jiang, *Adv. Mater.*, 2006, **18**, 3063–3078; (*g*) M. L. Ma and R. M. Hill, *Curr. Opin. Colloid Interface Sci.*, 2006, **11**, 193–202; (*h*) A. Nakajima, K. Hashimoto and T. Watanabe, *Monatsh. Chem.*, 2001, **132**, 31–41; (*i*) D. Quere, *Rep. Prog. Phys.*, 2005, **68**, 2495–2532; (*j*) C. Extrand, in *Encyclopedia of Surface and Colloid Science*, ed. P. Somasundaran, Taylor & Francis, New York, 2nd edn, 2006, pp. 5854–5868.
2 R. N. Wenzel, *Ind. Eng. Chem.*, 1936, **28, 8**, 988–994.
3 A. B. D. Cassie and S. Baxter, *Trans. Faraday Soc.*, 1944, **40**, 546–551.
4 T. Onda, S. Shibuichi, N. Satoh and K. Tsujii, *Langmuir*, 1996, **12**, 2125–2127.
5 X. Li, D. Reinhoudt and M. Crego-Calama, *Chem. Soc. Rev.*, 2007, **36**, 1350–1368.
6 W. Barthlott and C. Neinhuis, *Planta*, 1997, **202**(1), 1–8.
7 D. Quere, A. Lafuma and J. Bico, *Nanotechnology*, 2003, **14**(10), 1109–1112.
8 (*a*) N. J. Shirtcliffe, G. McHale, M. I. Newton and C. C. Perry, *Langmuir*, 2005, **21**(3), 937–943; (*b*) N. J. Shirtcliffe, S. Aqil, C. Evans, G. McHale, M. I. Newton, C. C. Perry and P. Roach, *J. Micromech. Microeng.*, 2004, **14**(10), 1384–1389.
9 (*a*) H. Kusumaatmaja and J. Yeomans, *Langmuir*, 2007, **23**(11), 6019–6032; (*b*) W. Li and A. Amirfazli, *Adv. Colloid Interface Sci.*, 2007, **132**(2), 51–68; (*c*) A. Marmur, *Langmuir*, 2004, **20**(9), 3517–3519; (*d*) C. Extrand, *Langmuir*, 2002, **18**(21), 7991–7999; (*e*) B. He, J. Lee and N. Patankar, *Colloids Surf. A.*, 2004, **248**(1–3), 101–104; (*f*) L. Gao and T. McCarthy, *Langmuir*, 2006, **22**(14), 6234–6237; (*g*) E. Bormashenko, R. Pogreb, G. Whyman and M. Erlich, *Langmuir*, 2007, **23**(12), 6501–6503.
10 C. Neinhuis and W. Bathlott, *Ann. Bot.*, 1997, **79**, 667–677.
11 T. Wagner, C. Neinhuis and W. Barthlott, *Acta Zool.*, 1996, **77, 3**, 213–225.
12 N. J. Shirtcliffe, F. B. Pyatt, M. I. Newton and G. McHale, *J. Plant Physiol.*, 2000, **163**, 1193–1197.
13 (*a*) *US Trademark*, 2 613 850, 1999; (*b*) *German Trademark*, 39 958 441.2, 1999.
14 G. M. Zhang, J. Zhang, G. Y. Xie, Z. F. Liu and H. B. Shao, *Small*, 2006, **2**, 1440–1443.
15 S. Michielsen and H. J. Lee, *Langmuir*, 2007, **23, 11**, 6004–6010.
16 Y. Y. Liu, R. H. Wang, H. F. Lu, L. Li, Y. Y. Kong, K. H. Qi and J. H. Xin, *J. Mater. Chem.*, 2007, **17, 11**, 1071–1078.
17 T. Wang, X. Hu and S. Dong, *Chem. Commun.*, 2007, 1849–1851.
18 D. Parker, *US Pat.*, 2 386 259, 1945.
19 L. C. Gao and T. J. McCarthy, *Langmuir*, 2006, **22, 14**, 5969–5973.
20 (*a*) F. Zhu, J. Zhang and W. van Ooij, *Dongbei Daxue Xuebao, Ziran Kexueban*, 2002, **28**(4), 22–27, 33; (*b*) J. Zhang, P. France, A. Radomyselskiy, S. Datta, J. Zhao and W. van Ooij, *J. Appl. Polym. Sci.*, 2003, **88, 6**, 1473–1481.
21 W. A. Daoud, J. H. Xin and X. Tao, *J. Am. Ceram. Soc.*, 2004, **87, 9**, 1782–1784.
22 W. A. Daoud, J. H. Xin, Y. H. Zhang and C. L. Mak, *Thin Solid Films*, 2006, **515**, 835–837.
23 M. Ma, R. M. Hill, J. L. Lowery, S. V. Fridrikh and G. C. Rutledge, *Langmuir*, 2005, **21**, 5549–5554.
24 S. Agarwal, S. Horst and M. Bognitzki, *Macromol. Mater. Eng.*, 2006, **291**, 592–601.
25 M. Ma, M. Gupta, Z. Li, L. Zhai, K. K. Gleason and R. E. Cohen, *Adv. Mater.*, 2007, **19**, 255–259.
26 T. Ogawa, B. Ding, Y. Sone and S. Shiratori, *Nanotechnology*, 2007, **18, 16**, 165607.

27 J. Zheng, A. He, J. Li, J. Xu and C. C. Han, *Polymer*, 2006, **47**, 7095–7102.

28 N. Bolgen, Y. Z. Menceloglu, K. Acatay, I. Vargel and E. Piskin, *J. Biomater. Sci., Polym. Ed.*, 2005, **16**, 12, 1537–1555.

29 Y. A. Dzenis and D. H. Reneker, *Proc. Am. Soc. Compos., Tech. Conf.*, 1994, **9**, 657–65.

30 (a) G. Srinivasan and D. H. Reneker, *Polym. Int.*, 1995, **36**(2), 195–201; (b) A. E. Zachariades, R. S. Porter, J. Doshi, G. Srinivasan, D. H. Reneker and H. Darrell, *Polymer News*, 1995, **20**(7), 206–207.

31 E. J. Robinette, G. R. Palmese and R. Giuseppe, Abs. Pap. 228th ACS National Meeting, Philadelphia, American Chemical Society, Washington, DC, USA, 2004, PMSE–536.

32 H. R. Allcock, A. Singh and L. Steely, *Polym. Prepr. (Am. Chem. Soc., Div. Polym. Chem.)*, 2005, **46**(2), 603.

33 K. Acatay, S. Kazim, O. Eren, M. Cleva and Z. Y Menceloglu, Abs. Pap., 229th ACS National Meeting, San Diego, CA, United States, American Chemical Society, Washington, DC, USA, 2005, POLY–504.

34 A. Singh, L. Steely and H. R. Allcock, *Polym. Prepr. (Am. Chem. Soc., Div. Polym. Chem.)*, 2005, **46**(2), 599–600.

35 (a) M. L. Ma, V. Krikorian, J. H. Yu, E. L. Thomas and G. C. Rutledge, *Nano Lett.*, 2006, **6**, 2969; (b) V. Kalra, P. A. Kakad, S. Mendez, T. Ivannikov, M. Kamperman and Y. L. Joo, *Macromolecules*, 2006, **39**, 5453.

36 Y. Miyauchi, B. Ding and S. Shiratori, *Nanotechnology*, 2006, **17**, 5151.

37 M. Zhu, W. Zuo, H. Yu, W. Yang and Y. Chen, *J. Mater. Sci.*, 2006, **41**, 12, 3793–3797.

38 Y. Zhu, J. C. Zhang, J. Zhai, Y. M. Zheng, L. Feng and L. Jiang, *ChemPhysChem*, 2006, **7**, 336–341.

39 N. S. Martys and J. F. Douglas, *Phys. Rev. E: Stat., Nonlinear, Soft Matter Phys.*, 2001, **63**, 3, 031205.

40 N. J. Shirtcliffe, G. McHale, M. I. Newton, C. C. Perry and P. Roach, *Mater. Chem. Phys.*, 2007, **103**, 1, 112–117.

41 X. H. Li, G. Chen, Y. Ma, L. Feng and H. Zhao, *Polymer*, 2006, **47**, 506–509.

42 J. T. Han, X. R. Xu and K. W. Cho, *Langmuir*, 2005, **21**(15), 6662–6665.

43 M. Yamanaka, K. Sada, M. Miyata, K. Hanabusa and K. Nakano, *Chem. Commun.*, 2006, **21**, 2248–2250.

44 A. Nakajima, K. Abe, K. Hashimoto and T. Watanabe, *Thin Solid Films*, 2000, **376**(1–2), 140–143.

45 (a) A. V. Rao and M. M. Kulkarni, *Mater. Res. Bull.*, 2002, **37**(9), 1667–1677; (b) N. J. Shirtcliffe, G. McHale, M. I. Newton and C. C. Perry, *Langmuir*, 2003, **19**(14), 5626–5631.

46 H. Y. Erbil, A. L. Demirel, Y. Avci and O. Mert, *Science*, 2003, **299**(5611), 1377–1380.

47 N. Zhao, J. Xu, Q. D. Xie, L. H. Weng, X. L. Guo, X. L. Zhang and L. H. Shi, *Macromol. Rapid Commun.*, 2005, **26**, 1075–1080.

48 Z. Yuan, H. Chen, J. Tang, X. Chen, D. Zhao and Z. Wang, *Surf. Coat. Technol.*, 2007, **201**, 7138–7142.

49 L. Jiang and J. Zhai, *Angew. Chem., Int. Ed.*, 2004, **43**(33), 4338–4341.

50 L. Vogelaar, R. G. H. Lammertink and M. Wessling, *Langmuir*, 2006, **22**(7), 3125–3130.

51 P. H. Tung, S. W. Kuo, K. U. Jeong, S. Z. D. Cheng and C. F. Huang, *Macromol. Rapid Commun.*, 2007, **28**(3), 271–275.

52 H. F. Hou and Y. Q. Chen, *J. Sol–Gel Sci. Technol.*, 2007, **43**(1), 53–57.

53 E. Hosono, S. Fujihara, I. Honma and H. Zhou, *J. Am. Chem. Soc.*, 2005, **127**(39), 13458–13459.

54 F. Shi, Y. Y. Song, H. Niu, X. H. Xia, Z. Q. Wang and X. Zhang, *Chem. Mater.*, 2006, **18**, 5, 1365–1368.

55 J. T. Han, Y. Jang, D. Y. Lee, J. H. Park, S.-H. Song and D.-Y. Ban, *J. Mater. Chem.*, 2005, **15**, 3089–3092.

56 A. C. Chen, X. S. Peng, K. Koczkur and B. Miller, *Chem. Commun.*, 2004, **17**, 1964–1965.

57 T. Ishizaki, N. Saito, Y. Inoue, M. Bekke and O. Takai, *J. Phys. D: Appl. Phys.*, 2007, **40**, 1, 192–197.

58 S. Shibuchi, T. Onda, N. Satoh and K. Tsujii, *J. Phys. Chem.*, 1996, **100**, 19512–19517.

59 R. Mohammadi, J. Wassink and A. Amirfazli, *Langmuir*, 2004, **20**, 9657–9662.

60 W. J. Fang, H. Mayama and K. Tsujii, *J. Phys. Chem. B*, 2007, **111**(3), 564–571.

61 H. Tavana, A. Amirfazli and A. W. Neumann, *Langmuir*, 2006, **22**, 5556–5559.

62 J. L. Zhang, J. A. Li and Y. C. Han, *Macromol. Rapid Commun.*, 2004, **25**, 1105–1108.

63 (a) K. Tsujii, T. Yamamoto, T. Onda and S. Shibuichi, *Angew. Chem., Int. Ed. Engl.*, 1997, **36**, 1011–1012; (b) S. Shibuichi, T. Yamamoto, T. Onda and K. Tsujii, *J. Colloid Interface Sci.*, 1998, **208**, 287–294.

64 X. J. Feng, L. Feng, M. H. Jin, J. Zhai, L. Jiang and D. B. Zhu, *J. Am. Chem. Soc.*, 2004, **126**, 62–63.

65 Y. H. Hyang, Z. Y. Li, B. Wang, C. X. Wang, D. H. Chen and G. W. Yang, *J. Phys.: Condens. Matter*, 2005, **17**, 5441–5446.

66 S. P. Tee, T. Shibata, H. Irie and K. Hashimoto, Fundamental Science and Technology of Photofunctional Interfaces, South Pacific, Proceedings of the 206th Meeting of the Electrochemical Society, ECS, Inc., 2004.

67 (a) R. Wang, K. Hashimoto, A. Fujishima, M. Chikuni, E. Kojima, A. Kitamura, M. Shimohigoshi and T. Watanabe, *Nature*, 1997, **388**, 431–432; (b) X. J. Feng, J. Zhai and L. Liang, *Angew. Chem., Int. Ed.*, 2005, **44**, 5115–5118.

68 W. Zhu, X. Feng, L. Feng and L. Jiang, *Chem. Commun.*, 2006, 2753–2755.

69 G. R. J. Artus, S. Jung, J. Zimmermann, H-P. Gautschi, K. Marquardt and S. Seegar, *Adv. Mater.*, 2006, **18**, 2758–2762.

70 X. D. Wu, L. J. Zheng and D. Wu, *Langmuir*, 2005, **21**, 2665–2667.

71 (a) I. P. Parkin and R. G. Palgrave, *J. Mater. Chem.*, 2005, **15**, 1689–1695; (b) S. Ashraf, C. S. Blackman, G. Hyett and I. P. Parkin, *J. Mater. Chem.*, 2006, **16**, 3575–3582.

72 X. Y. Lu, C. C. Zhang and Y. C. Han, *Macromol. Rapid Commun.*, 2004, **25**, 1606–1610.

73 K. K. S. Lau, J. Bico, K. B. K. Teo, M. Chhowalla, G. A. J. Amaratunga, W. I. Milne, G. H. McKinley and K. K. Gleason, *Nano Lett.*, 2003, **3**, 1701–1705.

74 (a) C. Journet, S. Moulinet, C. Ybert, S. T. Purcell and L. Bocquet, *Europhys. Lett.*, 2005, **71**, 104–9; (b) L. Huang, S. P. Lan, H. Y. Yang, E. S. P. Leong, S. F. Yu and S. Prawer, *J. Phys. Chem. B*, 2005, **109**, 7746–7748.

75 C. H. Chen, Q. J. Cai, C. L. Tsai, C. L. Chen, G. Y. Xiong, Y. Yu and Z. F. Ren, *Appl. Phys. Lett.*, 2007, **90**(17), 173108.

76 H. Liu and L. Jiang, *Soft Matter*, 2006, **2**, 811–21.

77 M. H. Jin, X. J. Feng, L. Feng, T. L. Sun, J. Zhai, T. J. Li and L. Jiang, *Adv. Mater.*, 2005, **17**, 1977–1981.

78 E. Balaur, J. M. Macak, H. Tsuchiya and P. Schmuki, *J. Mater. Chem.*, 2005, **15**, 4488–4491.

79 Z. Guo, F. Zhou, J. Hao and W. Liu, *J. Colloid Interface Sci.*, 2006, **303**, 298–305.

80 T. Baldacchini, J. E. Carey, M. Zhou and E. Mazur, *Langmuir*, 2006, **22**, 4917–4919.

81 L. M. Lacroix, M. Lejeune, L. Ceriotti, M. Kormunda, T. Meziani, P. Colpo and F. Rossi, *Surf. Sci.*, 2005, **592**(1–3), 182–188.

82 M.-F. Wang, N. Raghunathan and B. Ziaie, *Langmuir*, 2007, **23**, 2300–2303.

83 H. J. Busscher, I. Stokroos, H. C. Vandermei, P. G. Rouxhet and J. M. Schakenraad, *J. Adhes. Sci. Technol.*, 1992, **6**(3), 347–356.

84 H. J. Busscher, I. Stokroos, J. G. Golverdingen and J. M. Schakenraad, *Cells Mater.*, 1991, **1**(3), 243–249.

85 K. Teshima, H. Sugimura, Y. Inoue, O. Takai and A. Takano, *Langmuir*, 2003, **19**(25), 10624–10627.

86 K. Teshima, A. Takano, M. Akada, Y. Inoue, H. Sugimura and O. Takai Osamu, *Hyomen Gijutsu*, 2005, **56**(9), 524–527.

87 N. Vourdas, A. Tserepi and E. Gogolides, *Nanotechnology*, 2007, **18**, 125304.

88 M. Narita, T. Kasuga and A. Kiyotani, *Keikinzoku*, 2000, **50**(11), 594–597.

89 B. Qian and Z. Shen, *Langmuir*, 2005, **21**(20), 9007–9009.

90 X. Zhang, M. Jin, Z. Liu, S. Nishimoto, H. Saito, T. Murakami and A. Fujishima, *Langmuir*, 2006, **22**(23), 9477–9479.

91 M. Qu, B. Zhang, S. Song, L. Chen, J. Zhang and X. Cao, *Adv. Funct. Mater.*, 2007, **17**, 593–596.

92 M. Wang, N. Raghunathun and B. Ziaie, *Langmuir*, 2007, **23**, 2300–2303.

93 A. W. Hassel, S. Milenkovic, U. Schurmann, H. Greve, V. Zaporojtchenko, R. Adelung and F. Faupel, *Langmuir*, 2007, **23**(4), 2091–2094.

94 T.-Y. Kim, B. Ingmar, K. Bewilogua, Oh. K. Hwan and K.-R. Lee, *Chem. Phys. Lett.*, 2007, **436**, 199–203.

95 A. K. Geim, S. V. Dubonos, I. V. Grigorieva, K. S. Novoselov and A. A. Zhukov, *Nat. Mater.*, 2003, **2**, 461–463.

96 A. Satyaprasad, V. Jain and S. K. Nema, *Appl. Surf. Sci.*, 2007, **253**, 12, 5462–5466.

97 S. Karuppuchamy and J. M. Jeong, *Mater. Chem. Phys.*, 2005, **93**, 251–254.

98 N. J. Shirtcliffe, P. Thiemann, M. Stratmann and G. Grundmeier, *Surf. Coat. Technol.*, 2001, **142**, 1121–1128.

99 (a) A. Hozumi and O. Takai, *Thin Solid Films*, 1997, **303**(1–2), 222–225; (b) M. M. Bonnar, B. M. Burnside, A. Little, R. L. Reuben and J. I. B. Wilson, *Chem. Vap. Deposition*, 1997, **3**(4), 201–207.

100 J. P. Youngblood and T. J. McCarthy, *Macromolecules*, 1999, **32**(20), 6800–6806.

101 R. Brady and R. Ball, *Nature*, 1984, **309**, 225–229.

102 M. Li, J. Zhai, H. Liu, Y. L. Song, L. Jiang and D. B. Zhu, *J. Phys. Chem. B*, 2003, **107**(37), 9954–9957.

103 Y. G. Jiang, Z. Q. Wang, X. Yu, F. Shi, H. P. Xu and X. Zhang, *Langmuir*, 2005, **21**(5), 1986–1990.

104 L. B. Xu, W. Chen, A. Mulchandani and Y. S. Yan, *Angew. Chem., Int. Ed.*, 2005, **44**(37), 6009–6012.

105 J. Fresnais, J. P. Chapel and F. Poncin-Epaillard, *Surf. Coat. Technol.*, 2006, **200**(18–19), 5296–5305.

106 S. H. Kim, J. H. Kim, B. K. Kang and H. S. Uhm, *Langmuir*, 2005, **21**(26), 12213–12217.

107 I. A. Larmour, S. E. J. Bell and G. C. Saunders, *Angew. Chem., Int. Ed.*, 2007, **46**(10), 1710–1712.

108 Y. Y. Wu, N. Saito, F. A. Nae, Y. Inoue and O. Takai, *Surf. Sci.*, 2006, **600**(18), 3710–3714.

109 L. L. Yang, S. Bai, D. S. Zhu, Z. H. Yang, M. F. Zhang, Z. F. Zhang, E. Q. Chen and W. Cao, *J. Phys. Chem. C*, 2007, **111**(1), 431–434.

110 Y. J. Tang, X. H. Xu, J. Fang, Y. Liang and H. F. Ji, *IEEE Trans. Nanotechnol.*, 2006, **5**(4), 415–419.

111 G. L Cui, W. Xu, X. H. Zhou, X. W. Xiao, L. Jiang and D. B. Zhu, *Colloids Surf., A*, 2006, **272**(1–2), 63–67.

112 S. C. Cho, Y. C. Hong and H. S. Uhm, *J. Mater. Chem.*, 2007, **17**(3), 232–237.

113 S. Tsuruta, K. Morimoto, T. Hirotsu and H. Suzuki, *Jpn. J. Appl. Phys.*, 2006, **45**(10B), 8502–8505.

114 D. Oner and T. J. McCarthy, *Langmuir*, 2000, **16**, 20, 7777–7782.

115 Z. Yoshimitsu, A. Nakajima, T. Watanabe and K. Hashimoto, *Langmuir*, 2002, **18**, 15, 5818–5822.

116 L. Zhu, Y. Y. Feng, X. Y. Ye and Z. Y. Zhou, *Sens. Actuators, A*, 2006, **130**, 595–600.

117 C. H. Choi and C. J. Kim, *Nanotechnology*, 2006, **17**, 21, 5326–5333.

118 R. M. Wagterveld, C. W. J. Berendsen, S. Bouaidat and J. Jonsmann, *Langmuir*, 2006, **22**, 26, 10904–10908.

119 L. Cao, H. H. Hu and D. Gao, *Langmuir*, 2007, **23**, 8, 4310–4314.

120 A. Kawai and H. Nagata, *Jpn. J. Appl. Phys.*, 1994, **33L**, 1283–1285.

121 C. Dorrer and J. Ruhe, *Langmuir*, 2006, **22**, 7652–7657.

122 D. L. Herbertson, C. R. Evans, N. J. Shirtcliffe, G. McHale and M. I. Newton, *Sens. Actuators, A*, 2006, **130–131**, 189–193.

123 S. S. Guo, M. H. Sun, J. Shi, Y. J. Liu, W. H. Huang, C. Combellas and Y. Chen, *Microelectron. Eng.*, 2007, **84**, 1673.

124 E. Martines, K. Seunarine, H. Morgan, N. Gadegaard, C. D. W. Wilkinson and M. O. Riehle, *Nano Lett.*, 2005, **5**, 2097.

125 R. Furstner, W. Barthlott, C. Neinhuis and P. Walzel, *Langmuir*, 2005, **21**, 956.

126 A. Pozzato, s. Dal Zilio, G. Fois, D. Vendramin, G. Mistura, M. Belotti, Y. Chen and M. Natali, *Microelectron. Eng.*, 2006, **83**(4–9), 884–888.

127 S. Lee and T. H. Kwon, *J. Micromech. Microeng.*, 2007, **17**, 687–692.

128 Y. Li, X. J. Huang, S. H. Heo, C. C. Li, Y. K. Choi, W. P. Cai and S. O. Cho, *Langmuir*, 2007, **23**(4), 2169–2174.

129 C. Sun, L. Q. Ge and Z. Z. Gu, *Thin Solid Films*, 2007, **515**, 11, 4686–4690.

130 P. S. Tsai, Y. M. Yang and Y. L. Lee, *Langmuir*, 2006, **22**(13), 5660–5665.

131 J. Y. Shiu, C. W. Kuo, P. L. Chen and C. Y. Mou, *Chem. Mater.*, 2004, **16**, 561–564.

132 L. Zhu and Y. Jin, *Appl. Surf. Sci.*, 2007, **253**, 3432–3439.

133 J. X. Wang, Y. Q. Wen, J. P. Hu, Y. L. Song and L. Jiang, *Adv. Funct. Mater.*, 2007, **17**(2), 219–225.

134 J. X. Wang, Y. Q. Wen, X. J. Feng, Y. L. Song and L. Jiang, *Macromol. Rapid Commun.*, 2006, **27**(3), 188–192.

135 (a) W. Ming, D. Wu, R. van Benthem and G. de With, *Nano Lett.*, 2005, **5**(11), 2298–2301; (b) X. Liu and J. He, *J. Colloid Interface Sci.*, 2007, **314**(1), 341–345.

136 Y. H. Xiu, L. B. Zhu, D. W. Hess and C. P. Wong, *Langmuir*, 2006, **22**(23), 9676–9681.

137 M. Motornov, R. Sheparovych, R. Lupitskyy, E. MacWilliams and S. Minko, *J. Colloid Interface Sci.*, 2007, **310**(2), 481–488.

138 G. Zhang, D. Y. Wang, Z. Z. Gu and H. Mohwald, *Langmuir*, 2005, **21**(20), 9143–9148.

139 L. Zhai, F. C. Cebeci, R. E. Cohen and M. F. Rubner, *Nano Lett.*, 2004, **4**, 1349.

140 (a) J. Bravo, L. Zhai, Z. Wu, R. E. Cohen and M. F. Rubner, *Langmuir*, 2007, **23**(13), 7293–7298; (b) L. Zhang, H. Chen, J. Sun and J. Shen, *Chem. Mater.*, 2007, **19**, 948–953.

141 J. T. Han, S. Kim and A. Karim, *Langmuir*, 2007, **23**(5), 2608–2614.

142 T. Ogawa, B. Ding, Y. Sone and S. Shiratori, *Curr. Opin. Colloid Interface Sci.*, 2006, **11**(6), 324–329.

143 J. Bico, C. Marzolin and D. Quere, *Europhys. Lett.*, 1999, **47**, 2, 220–226.

144 R. A. Singh, E. S. Yoon, H. J. Kim, J. Kim, H. E. Jeong and K. Y. Suh, *Mater. Sci. Eng., C*, 2007, **27**, 4, 875–879.

145 J. Li, J. Fu, Y. Cong, Y. Wu, L. J. Xue and Y. C. Han, *Appl. Surf. Sci.*, 2006, **252**(6), 2229–2234.

146 E. Bormashenko, T. Stein, G. Whyman, Y. Bormashenko and R. Pogreb, *Langmuir*, 2006, **22**, 24, 9982–9985.

147 L. Zhang, Z. Zhou, B. Cheng, J. M. DeSimone and E. T. Samulski, *Langmuir*, 2006, **22**, 8576–8580.

148 L. Feng, Y. Song, J. Zhai, B. Liu, J. Xu, L. Jiang and D. Zhu, *Angew. Chem., Int. Ed.*, 2003, **42**, 7, 800–802.

149 W. Lee, M. K. Jin, W. C. Yoo and J. K. Lee, *Langmuir*, 2004, **20**, 7665–7669.

150 B. He, N. A. Patankar and J. Lee, *Langmuir*, 2003, **19**, 4999–5003.

151 H. Sun M, C. X. Luo, L. P. Xu, H. Ji, O. Y. Qi, D. P. Yu and Y. Chen, *Langmuir*, 2005, **21**, 8978–8981.

152 (a) P. Wagner, R. Fürstner, W. Barthlott and C. Neinhuis, *J. Exp. Bot.*, 2003, **54**, 385, 1295–1303; (b) B. Bhushan and Y. C. Jung, *Nanotechnology*, 2006, **17**, 2758–2772.

153 S.-M. Lee, H. S. Lee, D. S. Kim and T. H. Kwon, *Surf. Coat. Technol.*, 2006, **201**, 553–559.

154 J. C. Love, B. D. Gates, D. B. Wolfe, K. E. Paul and G. M. Whitesides, *Nano Lett.*, 2002, **2**(8), 891–894.

155 M. E. Abdelsalam, P. N. Bartlett, T. Kelf and J. Baumberg, *Langmuir*, 2005, **21**(5), 1753–1757.

156 Y. Li, W. Cai, B. Cao, G. Duan, F. Sun, C. Li and L. Jia, *Nanotechnology*, 2006, **17**, 238–243.

157 S. Herminghaus, *Europhys. Lett.*, 2000, **52**, 165.

158 N. J. Shirtcliffe, G. McHale, M. I. Newton, G. Chabrol and C. C. Perry, *Adv. Mater.*, 2004, **16**(21), 1929–1932.

159 L. C. Gao and T. J. McCarthy, *Langmuir*, 2006, **22**(7), 2966–2967.

160 Y. T. Cheng, D. E. Rodak, C. A. Wong and C. A. Hayden, *Nanotechnology*, 2006, **17**(5), 1359–1362.

161 M. Nosonovsky, *Langmuir*, 2007, **23**(6), 3157–3161.

162 S. T. Wang, Y. L. Song and L. Jiang, *Nanotechnology*, 2007, **18**(1), 015103.

163 J. P. Liu, X. T. Huang, Y. Y. Li, K. M. Sulieman, X. He and F. L. Sun, *J. Mater. Chem.*, 2006, **16**(45), 4427–4434.

164 N. J.Shirtcliffe, G. McHale, M. I. Newton, C. C. Perry and F. B. Pyatt, *Appl. Phys. Lett.*, 2006, **89**(10), 104106.

165 W. L. Gore, *US Pat.*, 3 664 915, 1972.

166 J. Genzer and K. Efimenko, *Biofouling*, 2006, **22**(5), 339–360.